The Role of Chromatin Remodeling Enzymes in Prevention of CAG-Repeat Expansions

An honors thesis for the Department of Biology.

Stephen Walsh

Tufts University, 2014

Advisor: Dr. Catherine H. Freudenreich
In lab mentor: Dr. Nealia House

Freudenreich Laboratory
Department of Biology
Tufts University
200 Boston Ave., Suite 4738
Medford, MA 02155

Thesis Committee: Dr. Catherine H. Freudenreich, Dr. Sergei Mirkin, Dr. Nealia House

May 2014

Acknowledgements

Thank you to my committee member and academic advisor, Dr. Sergei Mirkin for his insightful comments and guidance relating to academics and research over the last two years.

Thank you to my research advisor and committee member Dr. Catherine Freudenreich for all her support and guidance in research over the last two years. In addition, I would like to thank her for allowing me to continue on this project over the summer, and for actively looking for funding for me to continue on this project. It's been one of the more meaningful experiences for me at Tufts to work in this lab, and I cannot express how grateful I am to Dr. Freudenreich for allowing it to happen.

I would like to give an enormous thanks to my in-lab mentor and committee member Dr. Nealia House for all of her wisdom and patience over the last two years. I have been very fortunate to have such an incredible role model and teacher as my mentor, and I cannot thank her enough for her investment in helping me develop as a scientist.

Thank you to members of the Freudenreich lab, Dr. Melissa Koch, Jennifer Nguyen, Simran Kaushal, Allen Su, and Elliot Philips for their help with experimental and intellectual questions, as well as being a fun and supportive group of people to work with.

I'd also like to thank Dr. Lorraine Pillus and Dr. Lorraine Symington for providing bacterial plasmids and yeast strains that were crucial to this project.

Finally, thank you to all my friends and family for the support in times of extensive data collection and thesis writing.

Table of Contents

Abstract

Expansions of CAG repeats, often caused by errors in DNA replication, repair, and recombination, can cause neurodegenerative diseases. However, organisms can employ a number of strategies in preventing genomic instability. Previous data in our lab suggests that acetylation of lysine residues H4-K12 and H4-K16 at CAG repeats is important in marking the DNA for repair, but the exact molecular mechanism of how these modifications affected repair fidelity remained unknown. This thesis explores the action of chromatin remodelers, hypothesized to be directly recruited to the acetylated residues through their bromodomain protein motif. Our data support that recruitment of the bromodomain-containing remodeling proteins Rsc2 and Bdf1 by the acetylation of H4-K16 facilitates DNA repair through a post-replicative repair pathway via gap-induced sister chromatid recombination (SCR). Additional evidence presented here identifies that this feature is unique to histone H4, and that CAG repeat maintenance is not affected by the acetylation state of other histone residues. By contributing data from this thesis with previous work in our lab, a novel model of dynamic H4 acetylation leading to high-fidelity DNA repair at CAG repeats has been elucidated.

Introduction

For this project, the contribution of chromatin remodeling enzymes in prevention of CAG-repeat expansions was studied. Furthermore, their contribution to sister-chromatid recombination (SCR), a form of post-replicative repair (PRR), was characterized. Additional studies for this project attempted to elucidate if specific residues on histone N-terminal tails were contributing to repeat stability and PRR repair pathways, possibly through interaction with the identified remodeling enzymes. From this data, a working model of post-replicative DNA repair at a CAG repeat was developed, and additional experimental evidence to support this model was gathered as part of this project. To provide a background on how this model was developed, this introduction summarizes information on trinucleotide repeats, histones, chromatin modifications, chromatin remodeling enzymes, PRR and SCR, and a novel model of chromatin dynamics during DNA repair at CAG repeats.

1. Trinucleotide Repeats

A *microsatellite* is a sequence of DNA with repeated nucleotide subunits, ranging from 2 to 5 base pairs per repeat (Turnpenny and Ellard 2005). The research in Dr. Catherine Freudenreich's laboratory focuses on the genomic stability and fragility of microsatellite regions, including CAG trinucleotide repeats, in the yeast *Saccharomyces cerevisiae*. Understanding the mechanisms behind repeat expansions could potentially aid the development of therapeutics for these diseases.

1.1 Trinucleotide Repeat Expansions contribute to disease

Microsatellite repeats can give rise to different diseases when expanded (reviewed by Mirkin 2007). The expanded regions can negatively affect DNA processing in replication, repair, and recombination pathways. The repeats that give rise to these diseases may differ both in their repeat subunit (number and composition of nucleotides per repeat) and the location of the repeat with respect to transcriptional components. These diseases include Huntington's diseases (CAG repeat expansions in coding regions), fragile X syndrome (expansions of CGG in the 5'-UTR region), different forms of myotonic dystrophies (tri-nucleotide or tetra-nucleotide repeat expansions in 3'-UTRs and introns), progressive myoclonic epilepsy 1(12bp repeat expansions in the promoter region), Friedrich's ataxia (GAA repeat expansions in introns), and various spinocerebellar ataxias (most of which are caused by CAG expansions in coding regions, though SCA 10 is caused by a ATTCT repeat expansion in an intron). All of these diseases show a dominant inheritance pattern and neurodegenerative symptoms (Mirkin 2007).

1.2 Trinucleotide Repeats form Stable Secondary Structures

The repetitive sequences can become kinetically trapped in non-B-DNA conformations, which results in a structural basis for these diseases. When exposed as single-stranded DNA during processes of replication, repair, or recombination, the repeats may form thermodynamically stable secondary structures. These structures include hairpins, cruciforms, triplex H-DNA, i-motifs, e-motifs, and quadruplexes (McMurray 1999). The specific structure that is formed is dependent on the repeat sequence itself; for example, GC-rich sequence runs can form quadruplexes, AT-rich inverted repeats can form cruciforms, and CNG-repeats (where

N is any nucleotide) can form hairpins (Mirkin 2007). A visual representation of these structures is shown in Figure 1.

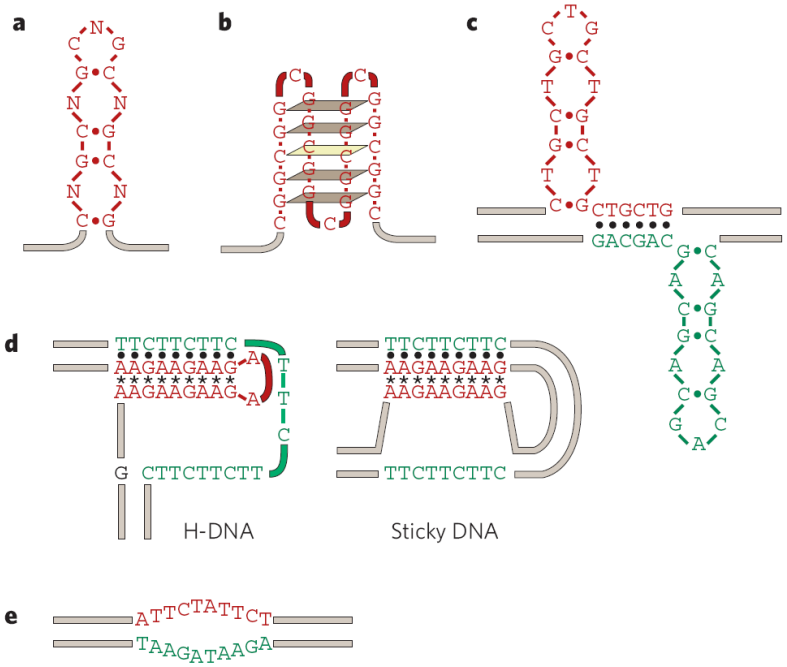

Figure 1. Repetitive DNA can form stable, non-B-DNA secondary structures
Repetitive DNA sequences can form alternative secondary structures in a sequence-specific, length-dependent manner, such as a) hairpins, b) quadruplexes, c) slipped-strand structures, d) triplex DNA structures, or e) a DNA-unwinding element (adapted from Figure 2 in Mirkin 2007).

Processing of DNA when a deleterious secondary structure has formed can lead to expansions and contractions. These mutations occur through replication, repair, and recombination pathways. All of these processes involve single-stranded DNA, formed by dissociation of the DNA duplex. Upon strand separation of the DNA duplex, the stable secondary structures can form, leading to disruption of normal processing of DNA lesions, subsequently resulting in expansions and contractions. Models for replication-driven expansions and contractions include strand slippage, errors in Okazaki fragment processing, and fork stalling (Lenzmeier and Freudenreich 2003), as well as fork reversal and template switching, where the

leading strand DNA polymerase loads onto the nascent lagging strand and continues synthesis off this new template. Upon synthesis of the full Okazaki fragment, a template switch back to the leading strand could result in expansions (Kim and Mirkin 2013).

In addition to forming secondary structures, an expanded repeat tract is also prone to breakage, or *chromosomal fragility*. When expanded repeat tracts are processed, there is an increased incidence of single-stranded nicks and gaps in the DNA. These nicks and gaps, or single stranded breaks (SSBs) may occur as a result of secondary structure formation (Freudenreich 2007). With only a single strand of the DNA duplex fully intact at the location of an SSB, breakage of the intact strand by DNA-damaging agents or erroneous DNA processing events can occur. This will convert the SSB into a full *double stranded break* (DSB). DSBs are particularly harmful to the cell, as the genetic material may be exposed to further degradation by nuclease activity, or erroneous recombination events can occur, leading to chromosome inversions, translocations, or duplications via error-prone processes such as non-homologous end-joining (NHEJ) (Freudenreich 2007).

2. DNA Processing in the Context of Chromatin

An important note to make about DNA processing of CAG-repeats in eukaryotes is that it occurs in the context of chromatin. Interestingly, CAG-repeats influence nucleosome positioning; through biochemical analysis and electron microscopy, expanded CAG-repeats have been found to be strong nucleosome assembly sites, which could interfere with transcription (Wang et al. 1994). This suggests that expanded CAG-repeats could disrupt normal chromatin assembly, and errors in chromatin assembly could contribute to CAG-repeat instability.

2.1 Histone Modifications

In addition to positional or structural modifications of nucleosomes (described in the next section), individual histones can be chemically modified. Histone proteins contain N-terminal or C-terminal tails that protrude from the nucleosome, allowing histone-modifying enzymes to access the tails. These tails are typically rich in lysine, arginine, serine, and threonine residues, giving the tails a strong polar character, typical in amino acids located on the outer portions of the protein (Costelloe et al. 2006). The amine and hydroxyl functional groups of lysine and serine, respectively, are of particular significance, as they are the chemical platforms where post-translational modifications (PTMS) can occur.

Histones can be chemically modified in a number of ways, including phosphorylation, acetylation, ubiquitination, and methylation. *Histone acetyltransferases* (HATs) are enzymes that add acetyl groups to N-terminal tail lysine residues (Millar and Grunstein 2006). The acetylation event is thought to neutralize the positive charge of the lysine residues, thus weakening the electrostatic interaction between histone proteins and DNA, promoting the more accessible euchromatic state of chromatin.

Histone acetylation is carried out by two main acetylation complexes in yeast: NuA4, which mainly targets histone H4, and the SAGA complex, which mainly targets histone H3 (Durant and Pugh 2007). The NuA4 complex is of particular interest in this study, due to its association with chromatin remodeler complexes such as SWR1 (Krogan et al. 2004). In fact, acetylation of H4 and H2A by NuA4 stimulates SWR1 to exchange histone H2A for histone variant H2A.Z (Altaf et al. 2010).

The acetyltransferase activity of NuA4 is carried out by the protein subunit Esa1. This subunit is essential for growth in yeast and deletion of the protein is lethal to the cell (Smith et al.

1998). For this reason, studies of NuA4 and Esa1 have used non-lethal *esa1* mutations; in this study, we used an *esa1-1851* allele that is catalytically dead, but still allows for viability. This *esa1-1851* allele is a mutation from cysteine to serine at amino acid 304, rendering it catalytically-dead in their H4 acetylation and DSB repair function (Decker et al. 2008). The loss of H4 acetylation function in this allele was demonstrated by a western blot for acetylated-H4, hypersensitivity to DSB-inducing agent MMS, and lethality at 37°C. The cysteine at position 304, along with Glu338, is thought to act in a "ping-pong" mechanism with an amino-acetyl intermediate during catalysis (Decker et al. 2008). Previous data in the Freudenreich lab indicated that Esa1 contributes to repeat stability. Using a yeast strain with the *esa1-1851* allele, a significant increase in expansions was observed as a 10-fold increase over wild-type (p-value = 0.005, data collected by Jiahui Yang).

Outside of its Esa1 function, other components of the NuA4 complex could play a role in repeat maintenance. The Yng2 subunit of the NuA4 complex has been found to play a role in the DNA damage response during S-phase and *yng2*Δ deletion mutants have been shown to be viable, but deficient in H4 acetylation (Choy and Kron 2002). Yng2 also plays an indirect role in localizing NuA4 to the histone for acetylation, by which it positions the active site of Esa1 to H4 and H2A N-terminal tails (Chittuluru et al. 2011). This suggests that the Yng2 protein is necessary for the integrity of the NuA4 complex itself, and any Yng2 deletion should mirror the *esa1-1851* in expansion phenotype.

Histone deacetylases (HDACs) are enzymes that remove acetyl groups from the histone N-terminal tails. Removal of acetyl groups promotes a heterochromatic state, meaning these proteins are strongly associated with gene silencing (Wang et al. 2002). For example, the HDAC Sir2 controls hypoacetylation states near telomere regions, where genes are rarely expressed

(Kimura et al. 2002). The HDAC Hos2 binds to coding regions following gene activation, deacetylating lysine residues in H3 and H4, thereby leading to subsequent gene inactivation (Wang et al. 2002). HDAC proteins have also been associated with DNA repair and genomic instability. For example, Sir2, Rpd3, and Hst1 appear two hours after an HO-endonuclease induced DSB, which coincides with a decrease in the acetylation state of chromatin flanking the break (Costelloe et al. 2006). Previous data collected by Dr. Jiahui Yang and Dr. Nealia House in the Freudenreich lab suggests that deletion of the HDAC proteins Hst1, Hos2, and Sir2 results in increased CAG repeat expansions, suggesting these proteins maintain repeat stability (unpublished). However, trinucleotide repeat expansions are found to be promoted by other HDAC proteins; in one study, mutations in the proteins Rpd3 and Hda1 suppressed up to 90% of expansions in yeast with a $(CTG)_{20}$ tract (Debacker et al. 2012).

The targeting of specific histone residues creates a complicated "histone code" which marks the chromatin to stimulate certain cellular processes, such as transcription, histone deposition during replication or orchestration of DNA repair (van Attikum and Gasser 2005). Specific histone acetylation marks in relation to DNA repair will be discussed later. A visual representation of chemically-modifying histone enzymes and their relevant N-terminal tail lysine residues is shown in Figure 2.

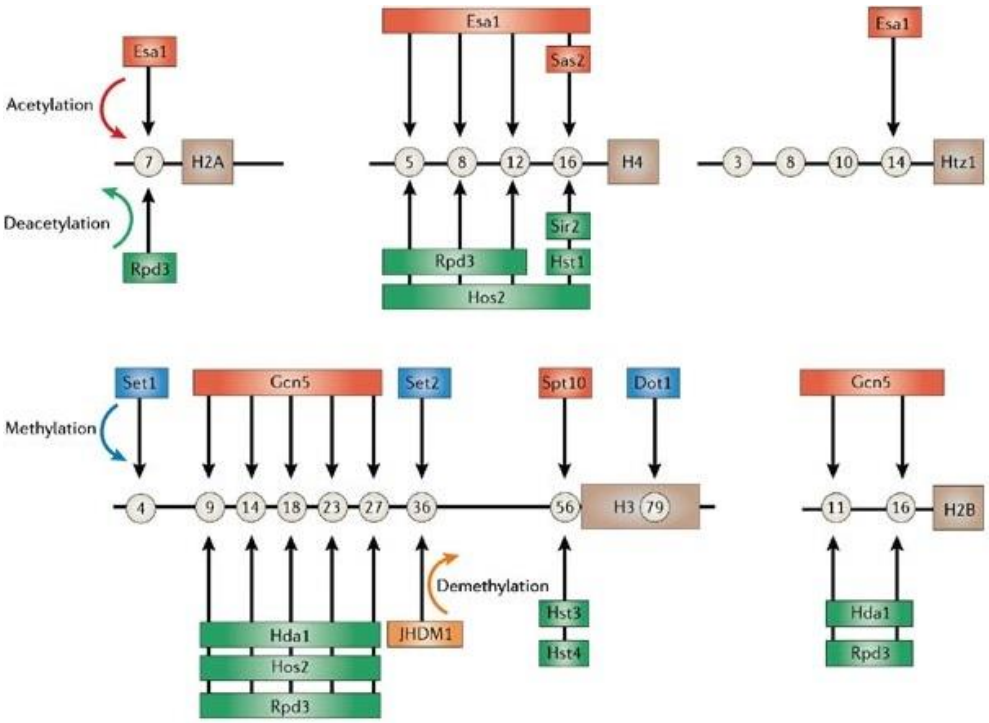

Figure 2. Histone N-terminal tail lysine residues are targeted for chemical modification in *Saccharomyces cerevisiae*
The lysine residues (numbers) on the N-terminal tails (left black lines) of histones H2A, H2B, H3, H4, and histone variant Htz1 are shown. Possible chemical modifications include acetylation by HATs (red), deacetylation by HDACs (green), methylation (blue), and demethylation (yellow). Each chemically-modifying enzyme has one or multiple specific residue targets (taken from Figure 1 in Millar and Grunstein 2006).

2.2 Chromatin Remodeling Enzymes

In addition to transcription, chromatin influences DNA replication and repair. In order to replicate or repair DNA, nucleosome assembly must be disrupted in order for the appropriate enzymes to access DNA unbound from nucleosomes. *Chromatin remodelers* are enzymes that carry out changes to nucleosome placement. These enzymes use ATP-hydrolysis to slide or evict nucleosomes, or participate in exchange of a histone subunit for another histone variant protein (Seeber et al. 2013).

This study focuses on three main remodeling complexes: the RSC, SWR1, and SWI/SNF remodeler complexes. The SWR1 complex functions at regions bordering heterochromatin and

euchromatin and promoter regions, depositing histone variant H2A.Z (or Htz1p, coded by the *HTZ1* gene in yeast) at the 5' ends of euchromatin genes (Raisner et al. 2008). The deposition of Htz1p at specific locations in the yeast genome has implied that SWR1 has specific roles in transcriptional gene regulation (Mizuguchi et al. 2004). SWR1 is driven by ATP-hydrolysis of the protein subunit Swr1, and has been found to physically interact with the NuA4 complex (Altaf et al. 2010). Yeast strains carrying mutations in *HTZ1, SWR1,* and various subunits of the NuA4 complex show defects in chromosome segregation (Krogan et al. 2004). These proteins may also play a role outside of transcriptional regulation; following UV-radiation, Htz1 plays a role in promoting H3 acetylation by HAT Gcn5, subsequently leading to nucleotide excision repair (Yu et al. 2013). Involvement of these proteins in DNA repair makes them candidates for investigation for their contribution CAG-repeat stability.

Another subunit of the SWR1 complex, Bdf1, is also of interest for this study. Bdf1 is a bromodomain-containing protein, found to interact with transcription factor II D (TFIID) and the SWR1 complex (Durant and Pugh 2007). Bdf1 has also been shown to bind tightly to histones when H4 residue K12 is acetylated, but is strongly inhibited from binding when residue K16 is acetylated (Millar et al. 2004). Since Bdf1 has the potential to bind and release from acetylated histones at different points in the repair process, a potential role in CAG-repeat maintenance was investigated for this project.

The SWI/SNF complex is a chromatin remodeling complex important in regulating transcription. The catalytic subunit of the complex, Snf2, is a bromodomain-containing protein that serves as the ATPase of the SWI/SNF complex (Chai et al. 2005). Additional studies by Chai et al. reveal that Snf2p is recruited to a DSB steadily over a 2 hour period post-DSB

induction. For these reasons, the Snf2 protein subunit was an attractive candidate for study in CAG repeat maintenance.

Of particular importance to this study is the *Remodeling the Structure of Chromatin*, or RSC complex. RSC has been shown to be necessary for cell viability, transcriptional regulation, chromosome transmission, sister-chromatid recombination, and was shown to play a role in dissociation of the invading strand from the donor strand during the post-synaptic stages of homologous recombination (Chai et al. 2005; Oum et al. 2011). ChIP studies have also shown that the RSC complex is present at replication forks in yeast (Niimi et al. 2012). Additionally, RSC has been shown to physically interact with the exonuclease Mre11, further suggesting a role in double strand break repair, as well as cohesin loading at breaks, suggesting a role in homologous recombination events (Costelloe et al. 2006).

The RSC complex appears in yeast in two different isoforms, different only in its bromodomain-containing subunit: Rsc1 or Rsc2 (Chambers et al. 2012). These two subunits are similar in structure (both contain two bromodomains), and deletion of either subunit results in cells defective in non-homologous end-joining (Chai et al. 2005). However, multiple studies have indicated that the two subunits have distinct roles with respect to other repair pathways. For example, a Rsc2 mutant showed hypersensitivity to the DSB-inducing agents MMS and CPT, while a Rsc1 mutant did not show such a phenotype (Chambers et al. 2012). A deletion of the *RSC2* gene resulted in reduced levels of PCNA ubiquitination, but this effect was not observed in a *RSC1* knockout (Niimi et al. 2012). Taken together, these results suggest that the isoform of the RSC complex containing the Rsc1 subunit could have more of a role in double strand break repair, whereas the isoform containing the Rsc2 subunit could have more of a role in post-replicative repair pathways, which are signaled by PCNA ubiquitination (Niimi et al. 2012).

2.3 Acetylated Histones can interact with chromatin remodelers through bromodomains

One protein motif common to many chromatin remodeling enzymes is the *bromodomain*. The bromodomain is a highly conserved protein structural component, consisting of four left-handed, antiparallel alpha-helices stabilized by a hydrophobic core (Horn and Peterson 2001). Proteins containing bromodomains are able to bind acetylated-lysine residues, specifically lysine residues located on the protruding N-terminal tails of histone proteins. The acetyl-lysine epitopes are recognized within the hydrophobic cavity of the bromodomain, where the acetylated-lysine can hydrogen bond with a conserved asparagine residue, anchoring it to the protein substrate (Filippakopoulos and Knapp 2012).

Ligand specificity and affinity of bromodomain-containing protein complexes differs between lysine residues along H3 and H4 N-terminal tails. It is thought that the residues flanking either side of the N-terminal lysine target could have specific interactions on the bromodomain core that stabilize the binding of the acetyl-lysine residue. For example, in humans, the P/CAF acetyltransferase targets residue K50 on the trans-activation protein Tat, which is stabilized by a downstream tyrosine interacting with Y802 and V763 on the P/CAF bromodomain (Zeng and Zhou 2002).

Bromodomain-containing proteins found in *Saccharomyces cerevisiae* are listed in Table 1. It is important to note that the proteins Rsc1, Rsc2 and Bdf1 contain two bromodomains each. The multiplicity has been studied in Rsc1 and Rsc2, with the finding that deletion of only the second bromodomain showed inhibition of growth (Zeng and Zhou 2002). For the purpose of this study, whole protein subunits were deleted for experiments. Chromatin remodeling subunits containing bromdodomains used in this study were Snf2, Rsc1, Rsc2, and Bdf1.

Table 1. Proteins in *Saccharomyces cerevisiae* with bromodomains
A list of all bromodomain-containing proteins in yeast is shown below. Proteins were found using the SMART protein database, with descriptions and bromodomain presence confirmed using the Saccharomyces Genome Database (created by Nealia House, 2013).

Protein	**Description**
Bdf1 (Bdf2)	Bdf1 is a basal transcription factor and SWR1 subunit. Bdf1 is redundant with Bdf2, and not required for SWR1 complex integrity or histone exchange activity (Wu et al, 2009).
Gcn5	HAT with lysine targets on H2B and H3. Gcn5 is a subunit of the RSC complex and a transcriptional regulator. It is also recruited to an HO-induced DSB (Tamburini & Tyler, 2005).
Snf2	The catalytic component of the SWI/SNF remodeling complex.
Spt7	A SAGA transcriptional regulation complex subunit that is required for complex assembly.
Sth1	Sth1 is the ATPase-containing subunit of the RSC complex. It is an essential helicase-related protein that is homologous to Snf2.
Rsc1	A component of the RSC remodeling complex that is required for nucleosome sliding flanking a DSB (Chambers et al, 2012).
Rsc2	A component of the RSC remodeling complex that may be associated with PRR (Niimi et al, 2012).
Rsc4	A component of the RSC remodeling complex that recognizes and binds to acetylated H3. Rsc4 is acetylated by Gcn5.

3. DNA Repair in Yeast

The yeast *Saccharomyces cerevisiae* has a similar chromatin assembly to that of humans. Since molecular mechanisms of chromatin, and DNA dynamics, are generally very similar across eukaryotes, this makes *S. cerevisiae* an ideal model organism to study DNA repair and other molecular phenomena.

3.1 Repair of double strand breaks in the context of chromatin

Of the different DNA repair pathways, the one that has been most extensively studied with respect to chromatin is double strand break repair (Seeber et al. 2013). The cascade of events that occur after inducing DSBs by an HO-endonuclease in yeast have been outlined by van Attikum and Gasser (2005). First, proteins Mre11, Rad50, and Xrs2 bind the DSB ends. This MRX complex processes the broken ends by 5' exonuclease activity, creating 3' ssDNA

overhangs. The chromatin remodeler complex INO80 has been shown to facilitate the end resection process by shifting nucleosomes away from the DSB end (Ataian and Krebs 2006). The MRX complex also serves to recruit the RSC complex via its association between RSC and Mre11 (Ataian and Krebs 2006). The action of RSC occurs mostly during later steps of homology-mediated repair of the DSB, including cohesin loading (Costelloe et al. 2006) as well as dissociation of the invading strand from the template strand during recombination (Chai et al. 2005).

Next, H2A C-terminal tail residue serine 129 becomes phosphorylated by protein kinases Tel1 and Mec1 (homologs to ATR kinases in humans). The dynamic enrichment of phosphorylated residues extends up to 50kb from the DSB in yeast (Shroff et al. 2005), and has been shown to extend up to 1Mb away from the break in humans (Lowndes and Toh 2005). Proteins recruited to phosphorylated H2A proteins include the remodeling complex INO80 and SWR1, and the NuA4 acetylation complex, all of which share a common phosphorylated-H2A binding subunit, Arp4 (Ataian and Krebs 2006). The NuA4 complex acetylates histone H3 and H4 residues in conjunction with chromatin remodeling by SWR1 and INO80. Following acetylation, homology-mediated repair can take place via invasion of the 3' ssDNA overhang. Once repair is complete, histone deacetylases, dephosphorylases, and chromatin remodelers work to return the DNA to its native chromatin assembly. This process seems to mediated by the protein factor CAF-1 and histone chaperone Asf1 (Ataian and Krebs 2006). A visual overview of chromatin dynamics during early repair of a double strand breaks is shown in Figure 3.

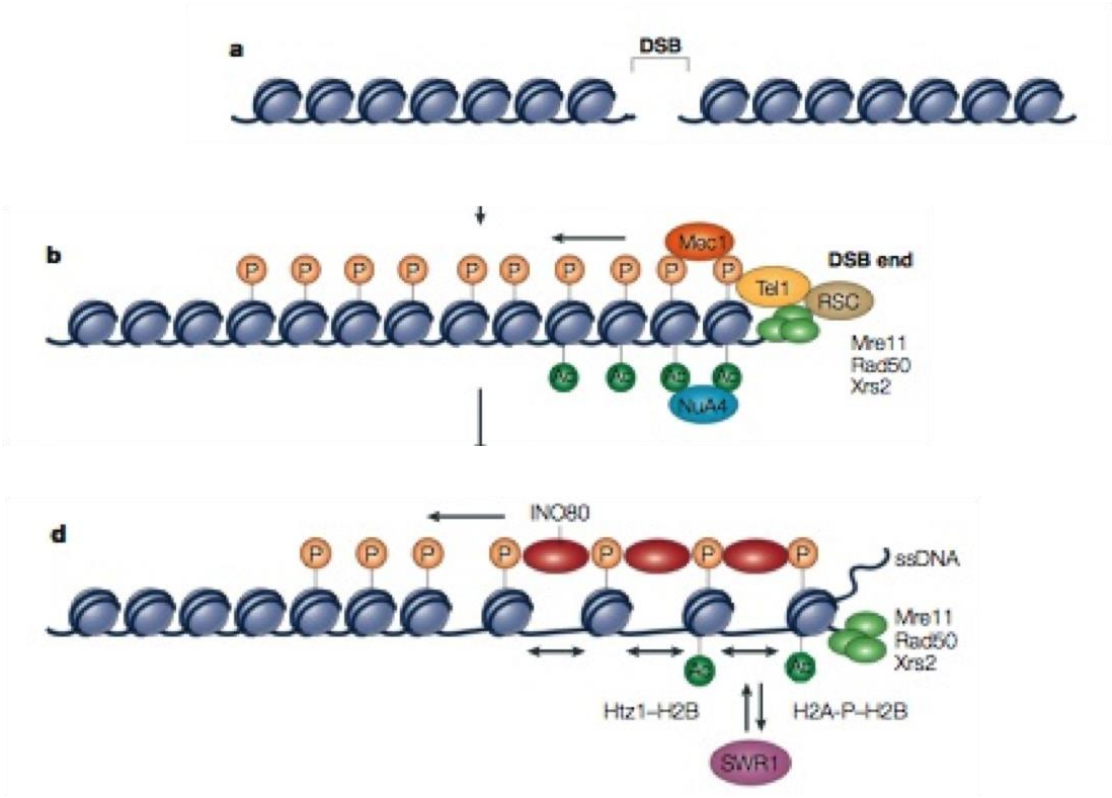

Figure 3. Double Strand Breaks in the Context of Chromatin
Upon induction of a DSB by an HO-endonuclease (a), end processing is carried out by the Mre11-Rad50-Xrs2 (MRX) complex. Phosphorylation of H2A is carried out by the Mec1 and Tel1 kinases, recruiting the NuA4 histone acetyltransferase complex. Histone PTMs further recruit chromatin remodeler complexes RSC, SWR1, and INO80, which facilitate DNA repair of the DSB (adapted from Figure 2 in van Attikum and Gasser, 2005).

3.2 Post-replicative Repair Pathways include Sister-Chromatid Recombination

When the replisome encounters a barrier on the DNA template (such as a tightly bound protein or a DNA hairpin), it may impair DNA synthesis leading to stalling of the replication fork. Alternatively, the fork can use mechanisms to proceed past the damage or re-prime downstream of the damage, leaving it to be repaired by post-replication repair (PRR, see below). A stalled replication fork can become deleterious to the cell, as it can lead to fork collapse, a double strand break, and other mutations if not remedied fast enough (van Attikum and Gasser 2005).

Post-replicative repair (PRR) refers to DNA repair pathways that occur as the replisome encounters a lesion or directly after replication. An overview of PRR has been described in eukaryotes by Andersen et al. (2008). In general, these PRR pathways can be grouped according to mechanism. Upon DNA damage, the preferred high-fidelity pathway in yeast is homologous recombination (Ataian and Krebs 2006). In yeast, mono-ubiquitination of residue K164 on the PCNA sliding clamp by the Rad6-Rad18 heterodimer results in recruitment of translesion synthesis (TLS) polymerases that can synthesize nucleotides over the lesion in an error-prone manner. Error-free bypass is possible by polyubiquitination of PCNA-K164 by the Mms2-Ubc13-Rad5 complex, which results in homology-mediated repair solutions: fork reversal or template-switch recombination (see Figure 4). This pathway promotes error-free DNA repair by synthesizing off of the sister strand in a transient template switch (Zhang and Lawrence 2005). The Rad5 protein is thought to mediate a pathway of HR-mediated repair by a poorly-understood template switch (Gangavarapu et al. 2013).

Repair of DNA at CAG-repeats requires high-fidelity repair pathways in order to prevent repeat instability. An HR-mediated repair pathway that has been implicated in repair near CAG-repeats is *sister chromatid recombination* (SCR) (Nag et al. 2004; Kerrest et al. 2009). SCR is dependent upon the protein Rad51, which forms a 3' invading nucleoprotein filament, and can be induced by DSBs, or more commonly, by single-stranded gaps formed at stalled replication forks (Mozlin et al. 2008). Additional proteins involved in SCR in yeast include the Rad51 paralogs Rad55 and Rad57, thought to stabilize the invading nucleofilament, as well as Rad52, which stimulates strand exchange (Kerrest et al. 2009).

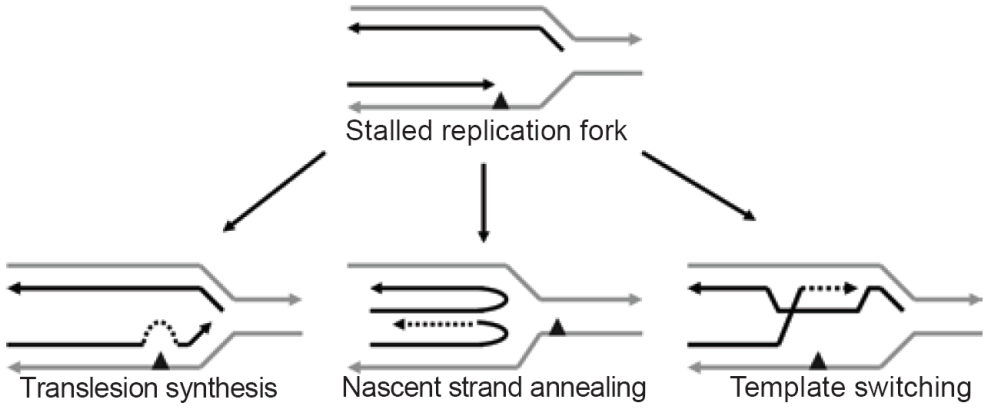

Figure 4. Post-Replicative Repair (PRR) Pathways
Upon encountering a DNA lesion, the replisome machinery stalls. The cell employs various strategies to overcome fork stalling, including error-prone translesion synthesis (left), fork reversal (middle), or error-free synthesis off the sister strand (right) (adapted from Andersen et al 2008).

4. A model for DNA repair at the CAG-repeat through dynamic H4 acetylation

Repair of DNA in several different pathways in the context of chromatin has been described in many scientific articles, with the most extensively described pathway being double strand break repair (Seeber et al. 2013). However, the influence of chromatin state during the repair of lesions at CAG repeats has not been extensively characterized. Therefore, the aim of this study was to better characterize DNA repair and chromatin dynamics at CAG repeats. The conclusions from this study allow us to present a novel model of chromatin dynamics during post-replication DNA repair at the CAG-repeat.

4.1 Previous H4 Acetylation Data Collected in the Freudenreich Lab

Prior to this study, data in the Freudenreich lab had pointed to specific HATs, HDACs, and lysine residues that contribute to CAG-repeat maintenance. As summarized in Figure 5, previous instability data collected by Jiahui Yang and Nealia House indicated that Esa1 contributes most to repeat maintenance among HATs, and among the HDAC proteins, Hst1,

Hos2, and Sir2 play the largest role in repeat maintenance. Together, this suggests a role of H4 acetylation in CAG repeat stability, since all of these proteins overlap in their targeting of H4 residues. This hypothesis was further confirmed by stability data of H3 and H4 N-terminal tail mutations. While the H3-NΔ mutant did not show a phenotype of CAG expansions, K to R mutations (which inhibits acetylation) on the H4 tail showed significant increases in expansion frequency, with the effect most pronounced upon mutation of residues K12 and K16.

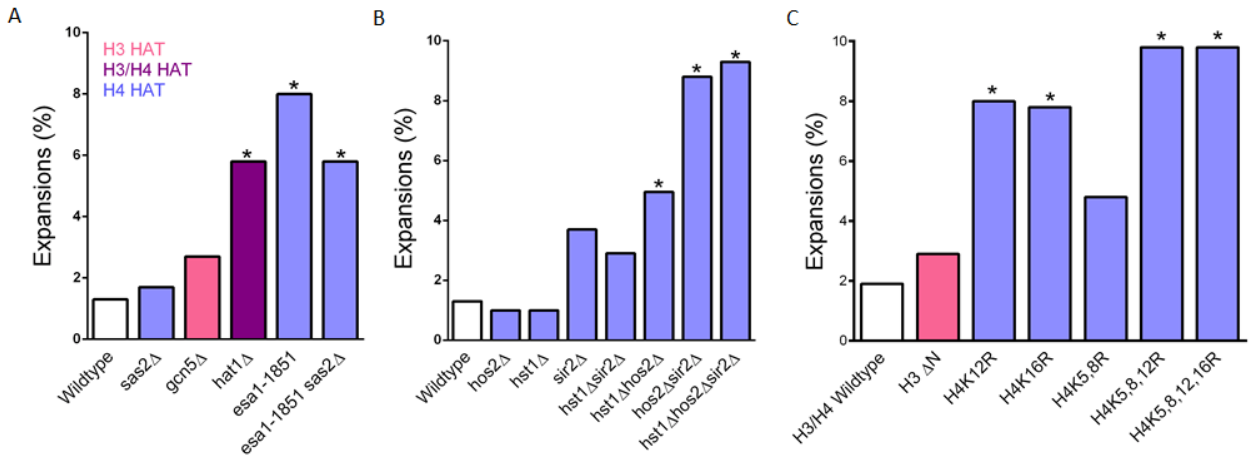

Figure 5. HAT and HDAC instability indicate role of histone H4 in repeat maintenance
Previous stability data indicates that H4-targeting HAT Esa1 (A) and H4-targeting HDACs Hst1, Hos2, and Sir2 (B) make the most significant contribution to CAG repeat maintenance. H4 acetylation, specifically at lysine residues H4-K12 and H4-K16, was also found to contribute to CAG repeat maintenance, while absence of H3 acetylation did not significantly increase repeat instability (C). An asterisk indicates expansion increase over wildtype to a p-value < 0.05 using Fisher's exact test. (data by Jiahui Yang and Nealia House, figures by Nealia House).

In addition to stability data, prior lab data also indicated SCR as contributing to repair at the CAG repeat. Mutant strains with deletions of proteins involved in PRR (Rad52, Rad5, and Rad57) were constructed in *esa1-1851* and *hst1*Δ*hos2*Δ*sir2*Δ strain background and tested for instability phenotypes (Figure 6). The double mutants all showed a suppression of expansions compared to the HAT and HDAC backgrounds, indicating that in the absence of proper Esa1 HAT and Hst1, Hos2, Sir2 HDAC activity, expansions were arising through processes dependent

on Rad5, Rad52, and Rad57 (e.g. PRR). The specific suppression of expansions seen in double mutants with Rad52, a protein involved in strand exchange (Kerrest et al., 2009), suggests that the PRR pathway involved is sister-chromatid recombination.

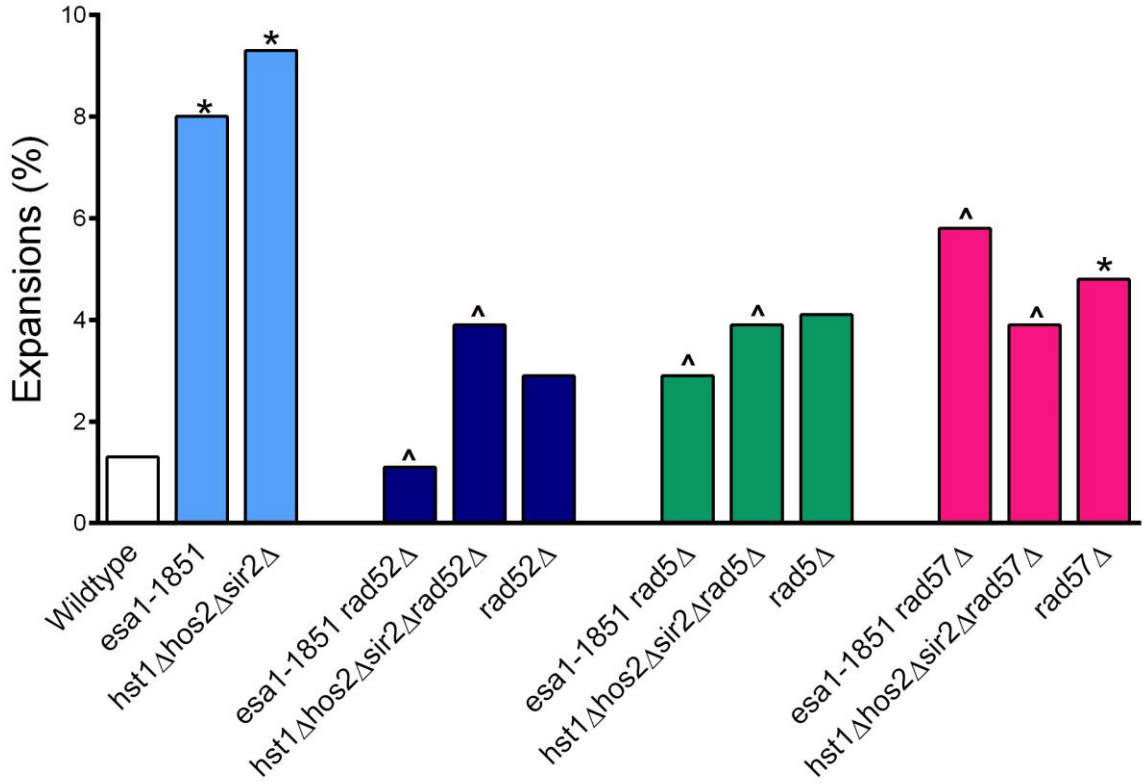

Figure 6. Expansions in HAT and HDAC mutants occurs during PRR processes
Suppression of expansions (indicated by an arrow) compared to HAT and HDAC mutants were observed when deletions of Rad5, Rad52, and Rad57 were made in these backgrounds. This suggests that expansions in the absence of proper HAT and HDAC activity at the CAG repeat arise through PRR processes. Strains were created by Yiahui Yang and Nealia House and stability assays were performed by Jiahui Yang and Nealia House.

4.2 Dynamic H4 Acetylation Promotes High-Fidelity DNA Repair at CAG-Repeats

To integrate these previous findings, a model was developed by which dynamic histone acetylation can lead to DNA repair of endogenous DNA lesions (see Figure 7; Yang, House, Freudenreich, submitted). Repair of such lesions, including gaps, nicks, or hairpins behind a replication fork, begins with binding of the NuA4 complex to phosphorylated histone H2A at the

CAG-repeat. The residue H4-K16 is acetylated by NuA4 to mark the lesion. The acetylated histones further recruit repair proteins employed in the sister chromatid recombination (SCR) pathway. Upon completion of SCR, HDAC proteins are recruited to modify chromatin to its prior deacetylated state, removing any chemical marks for DNA damage. This model suggests a high-fidelity pathway of repair, resulting in maintenance of CAG-repeat number. Without the H4-acetylation events, the appropriate proteins are not recruited, leading to compromised DNA repair and repeat expansions. On the other hand, in the absence of HDAC activity, a global H4-acetylation state results, which could result in inefficient targeting of the acetyl-binding proteins, and reduced resolution, thus contributing to CAG-repeat instability.

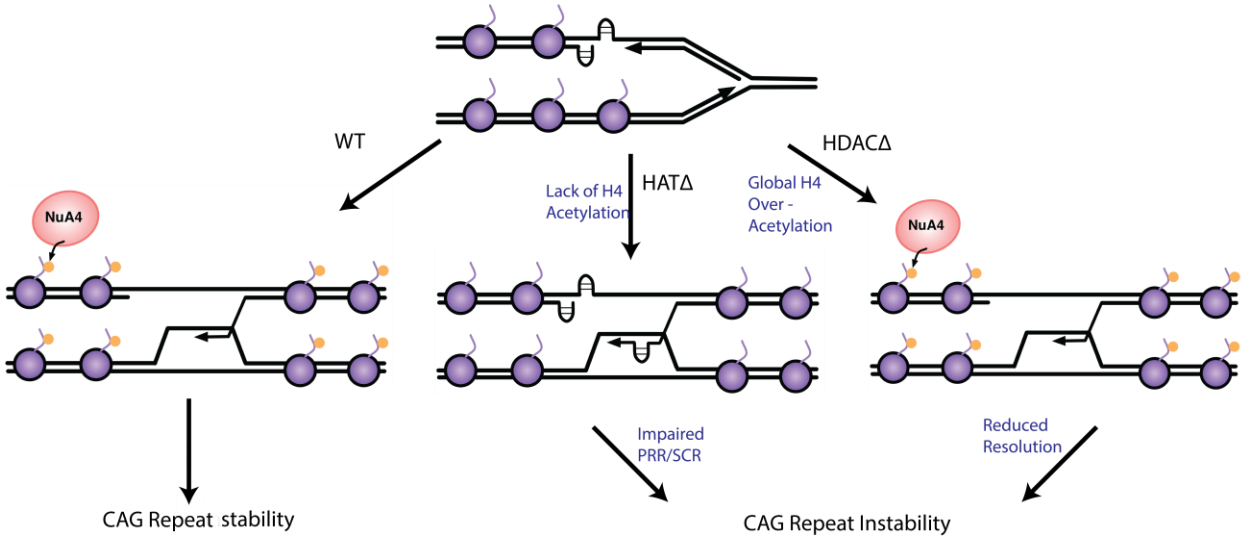

Figure 7. Dynamic H4 Acetylation Occur During PRR at the CAG Repeat
DNA lesions left behind a replication fork trigger H4 acetylation by the NuA4 complex. Once the histones are marked, high-fidelity pair takes place through sister chromatid recombination. Removal of acetyl groups by HDAC proteins marks the end of repair, leading to maintained repeat stability (left). Errors in this pathway, however, such as deletions of HAT (middle) and HDAC (right) activity, lead to impairments in the DNA repair process, and can lead to CAG repeat instability (adapted from House et al, submitted).

4.3 Goals of this thesis project

The model previously described indicates that acetylation of H4-K12 and H4-K16 occurs during PRR at the CAG repeat, and are important for high-fidelity repair. However, there was still one big question remaining from these studies: how do these modifications impact repair fidelity? From this main question, three more focused research questions were asked:

First, we hypothesized that upon these acetylation events, the modified histones could bind one or more bromodomain-containing proteins, and that the chromatin remodeling actions of these proteins could facilitate higher-fidelity repair during PRR. To test this hypothesis, various studies of bromodomain-containing remodeling proteins were carried out to see which, if any, of these proteins maintain repeat stability. Furthermore, if remodeling activity was found to play a role in maintaining CAG repeats, we explored whether or not their actions are epistatic with the HATs and HDACs suggested in this model.

Additionally, we wanted to further characterize if the high-fidelity repair events were specifically initiated by Esa1 acetylation of H4-K12 and H4-K16, or if acetylation of other histone proteins impacted repair fidelity. To test this, studies of additional histone acetylation targets with respect to CAG repeat stability were performed. The importance of Esa1 function to H4 acetylation, and subsequent repeat stability and SCR, via the NuA4 subunit Yng2, was also studied in the context of this model.

Finally, we asked whether or not the H4-K12 and H4-K16 acetylation events specifically contributed to sister chromatid recombination. A more focused research experiment involved constructing strains lacking H4-K12 and H4-K16 acetylation, which were subsequently studied to see if rates of SCR decreased in unacetylatable point mutants.

Materials and Methods

Mutant Yeast Strain Construction

Mutant *Saccharomyces cerevisiae* strains were created with deletions or mutations in the proteins of interest, by two-step gene replacement. An overview of the strain construction process is given in Figure 8, while all strains created for the purpose of this study are listed in Appendix B (Table B.1).

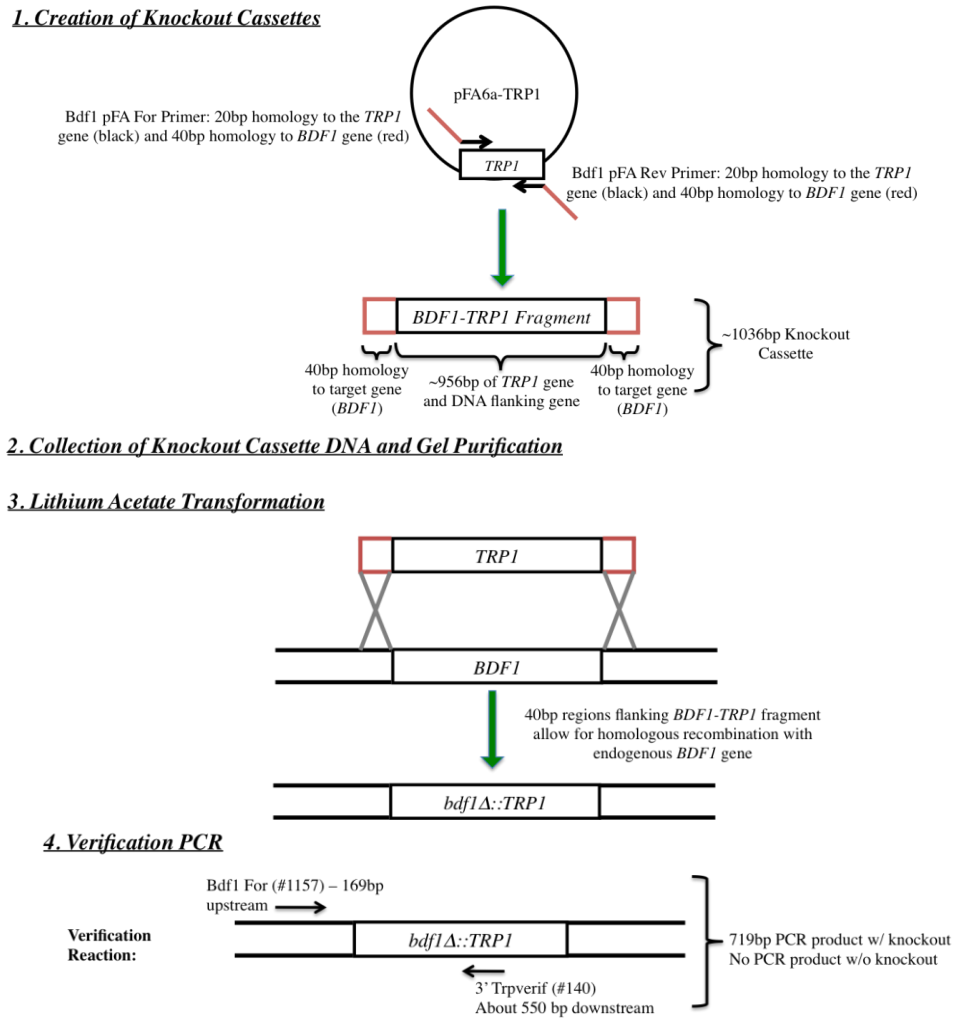

Figure 8. Experimental Design of Strain Construction
Shows a visual representation of how the knockout strains were prepared. The representation above uses the *BDF1* gene knocked out with TRP1 from the pFA6a-TRP1 plasmid template as an example. A genomic DNA template was used in the construction of *swr1*Δ and H4 point mutant SCR strains (not shown).

1. Bacterial Plasmid Mini-Preps for Desired Knockout Markers

To obtain plasmids for knockout cassette construction or plasmid shuffles, bacterial strains containing pFA-plasmids were cultured in an overnight process to harvest their plasmid DNA. Bacteria from a glycerol stock stored at -80°C was grown in 2mL of LB media with 100μg/mL ampicillin overnight at 37°C. From the 2mL culture, plasmid DNA was isolated using the Zyppy Plasmid Mini-Prep Kit by Zymo Research according to the manufacturer's instructions. Plasmids used in this study are listed in Table 2 and Table 3.

Table 2. pFA Plasmids templates for knockout cassette construction
Each plasmid is a pFA backbone, and therefore the upstream and downstream sequences relative to a yeast selectable marker are identical. Primers with homology to these sequences were used in order to construct knockout cassettes in a two-step gene replacement

Plasmid Name	**CF Plasmid / Bacterial Stock Number**	**Marker Used for Amplification**	**Desired PCR Product Size**
pFA6a-KanMX6	136	*KanMX6*	1560bp
pFA6a-TRP1	137	*TRP1*	1037bp
pFA6a-HisMX6	138	*HIS3*	1404bp

Table 3. Plasmids used in plasmid shuffle transformations
The plasmid shuffle transformation involves introducing a mutant allele of an essential gene via a *CEN* plasmid. The parent yeast strains used in these transformations contain an endogenous *CEN* plasmid with a selectable marker different than the plasmids listed below. Selection for the mutant plasmid should cause the endogenous plasmid to be lost while retaining the introduced ("shuffled") plasmid due to its different selectable marker and essential gene.

Plasmid Name	**CF Plasmid / Bacterial Stock**	**Plasmid Information**	**Mutant Strain to be Constructed**
H3/H4 wild-type	319	pRS314 backbone with *HHT2-HHF2* insert in multiple cloning site	H3/H4 wildtype SCR
H4-K12R	320	pRS314 backbone with *HHT2-hhf2-K12R* insert in multiple cloning site	H4-K12R SCR
H4-K16R	321	pRS314 backbone with *HHT2-hhf2-K16R* insert in multiple cloning site	H4-K16R SCR
pJH161-FB1550-H2A-NΔ	456	FB639 (pT52) derivative containing *HTB1, hta1*Δ(5-21) and *HIS3* (from Winston lab)	H2A-NΔ $(CAG)_{85}$
H4-K5,8,12Q	470	pRS314 backbone with *HHT2-hhf2-K5,8,12Q* (from Pillus lab)	H4-K5,8,12Q $(CAG)_{85}$

2. Yeast Genomic DNA Mini-Preps for Desired Knockouts with Increased Gene-Homology

Knockout cassettes used in yeast transformations for *swr1*Δ, H3/H4 wildtype SCR, H4-K12R SCR, and H4-K16R SCR strains were constructed using genomic DNA template from previously constructed strains that were not isogenic to the strains to the strains in this study (e.g. BY4741, Stanford Deletion Set) or had a different tract-length (e.g. CAG-70). Template strains are listed in Table 4. Genomic DNA was isolated following the Freudenreich lab protocol for genomic DNA preps (See "Yeast DNA MiniPreps" procedure page from CHF Lab Binder). Template strains were grown to stationary phase in 5mL of YEPD media at 30°C. DNA pellets were resuspended in 30µL 1X TE and stored at 4°C.

Table 4. Yeast strains used as genomic DNA templates
These strains already contained the desired gene knockout of interest, but in different strain background. Genomic DNA from these strains was isolated and used as a template (instead of a plasmid) for knockout cassette construction in a BY4705 $(CAG)_{85}$ strain background.

Template Strain	**CF Strain Number**	**Genotype Information**	**Mutant Strains to be Constructed**
*swr1*Δ*::KAN*	1468	BY4742, from Stanford Deletion Set	*swr1*Δ BY4705 $(CAG)_{85}$
H3/H4 wild-type	2051	*hht1hhf1*Δ*::HIS3, hht2hhf2*Δ*::KanMX6,* with H3/H4 wildtype plasmid (pRS314)	H3/H4 wildtype SCR H4-K12R SCR H4-K16R SCR

3. Creation of Knockout Cassettes:

In order to knockout specific genes of interest, PCR was used to create DNA knockout cassettes for preparation in the first step of two-step-gene replacement. PCR was performed using the Roche Expand High-Fidelity PCR kit protocol (See "Expand PCR" procedure page from CHF Lab Binder). For template DNA, 2µL of a 1:50 dilution of the appropriate plasmid, or 2µL of a 1:100 dilution of yeast genomic DNA was used along with 1.0µL of Roche 3.5 U Expand enzyme per reaction. The final volume for this PCR was 50µL per reaction. Forward

and reverse primers annealing to the plasmid were designed with 20bp homology to the plasmid plus 40bp "tails" corresponding to sequences directly flanking the start and stop codons of the gene of interest (see appendix Table A.1). When the template DNA was from a genomic prep, the forward and reverse primers used were between 50 to 300bp upstream or downstream of the knocked-out gene of interest (see appendix Table A.2).

In order to isolate plasmid-template PCR products from the plasmid template itself, a PCR clean-up step was required. The products from the Expand PCR reaction were precipitated and purified by adding a $1/10^{th}$ volume of 3M potassium acetate and an equal volume of 100% isopropanol. Products were mixed and centrifuged at 14,000 rpm for 30 minutes at 4°C. The supernatant was discarded and the DNA pellet was washed twice with 70% ethanol for one minute. The DNA pellet was dried at room temperature for 10 minutes and then resuspended in 10µL of 1X TE solution, to be used for gel purification.

PCR products made from a genomic DNA template were collected in the same procedure as previously described, except they were resuspended in 30µL 1X TE; gel purification of these products was not required.

If the products came from a plasmid-based template, a required gel purification step was performed. Gel purification of the plasmid-template PCR products began by loading the products onto a 1.5% agarose gel, ethidium bromide-stained gel. Electrophoresis was carried out at 95V for about 50 minutes and then visualized using UV-radiation. DNA bands of the appropriate size were excised from the gel and then gel purified using the Thermo Scientific GeneJET Gel Extraction Kit, following the manufacturer's instructions.

4. Lithium Acetate Transformations to Create Knockouts

In order to integrate the knockout cassette or mutant plasmid into yeast, transformations were used to introduce the foreign DNA. The starting parent strains used in these transformations are listed in Table 5. Transformations were performed using a lithium acetate protocol. A small inoculum of cells from patch was added to 2mL of either YC-Leu (for YAC-containing strains) or YEPD (no YAC strains) media and grown overnight at 30°C in a roller drum to stationary phase. The next day, 200 to 400µL of the culture solution was reinoculated into 10mL of fresh media, and grown at 30°C, 220 rpm in a floor shaker. Cells were then pelleted at 3000 rpm for 5 minutes, resuspended in 1mL deionized sterile H_2O, pelleted at 5000rpm for 1 minute, and resuspended in 1mL Transformation Solution A (800µL H_2O, 100µL 1X TE, 100µL 1M lithium acetate). Cells were pelleted once again, and resuspended in 100µL of Transformation Solution A. Next, 50µL of the cells, 10µL of 5X salmon sperm DNA (boiled in water for 5 minutes, cooled on ice for 1 minute), and 10 to 15µL of the transformation fragment (or 5 to 8µL of plasmid DNA for plasmid shuffles) were added to 300µL of Transformation Solution B (240µL 50% polyethylene glycol, 30µL 1X TE, 30µL 1M lithium acetate). The solution was mixed thoroughly and then placed at 30°C in a roller drum for 30 minutes for recovery. The cells were then mixed with 15µL of 100% DMSO and placed in a 42°C water bath for 15 minutes. Cells were then pelleted at 8000rpm for 2 minutes and resuspended in 1mL of YEPD media and transferred to a culture tube and incubated at 30°C in a roller drum. Transformations using a *TRP1* or *HIS3* marker were grown for 1 hour, while transformations using the *KanMX6* marker were grown for 2 hours.

After recovery, cells were pelleted at 5000 rpm for 2 minutes, washed once with diH_2O, plated on selectable media, and grown at 30°C for 3 to 5 days. Transformant colonies that grew

were re-patched onto a fresh selective plate and grown at 30°C for an additional 2 days. This added step ensured that any background growth would be excluded from further transformant verification PCR and stability analysis.

Table 5. Starting strains for transformation
In order to ensure consistency across each type of analysis (stability assays and SCR assays), the same parent strains were used in the construction process to have mutants that were isogenic to one another.

Parent Strain Name	Desired Mutant Strains	Strain Number	Genotype
BY4705 wild-type	*rsc1Δ, rsc2Δ, bdf1Δ, snf2Δ, swr1Δ, htz1Δ, yng2Δ,*	CFY810	Mat α, ade2Δ::hisG, his3Δ200, leu2Δ0, lys2Δ0, met15Δ0, trp1Δ63, ura3Δ0, YAC CF1 = *URA3, LEU2, ade3-2p,* $(CAG)_{85}$
esa1-1851	Esa1 HAT and chromatin remodeler double mutants (*rsc1Δ, rsc2Δ, bdf1Δ, snf2Δ*)	CFY2050	Same as CFY810; *esa1-1851* mutation = C304S; *KanMX6* at end of *ESA1* locus
hst1Δhos2Δsir2Δ	Triple HDAC and chromatin remodeler mutants (*rsc1Δ, rsc2Δ, bdf1Δ, snf2Δ*)	CFY2656	Same as CFY810; *hst1Δ::HIS3, hos2Δ::KanMX6; sir2Δ::Hph*
Wildtype SCR	*yng2Δ* SCR	CFY2867	LSY1519-1D; matα, ade2-nde1-::TRP1::ade2-I-Sce1+/aatII-; RAD5+, ade2-1 trp1-1 his3-11,15 can1-100 ura3-1 leu2-3,112
LSY1892	H3/H4 WT SCR, H4-K12R SCR, H4-K16R SCR	CFY3104	MATα, trp1-1, his3-11,15 can1-100 lue2-3,112 ade2-n-URA3-ade2-a RAD5
H4-K5,8R	H4-K5,8,12Q	CFY2757	BY4705, hht1hhf1::His, hht2hhf2::Kan, with H4-2KR plasmid (pRS314)
FY406	*H2A-NΔ*	CF1328	Mat a, LEU2, TRP1, ura3-52, lys2Δ, his3Δ200

5. Verification PCR using TaqCol to Confirm Transformants

Successful transformants had to be verified for correct integration of knockout cassettes at the desired locus. Verification of transformant strains was obtained using a colony PCR (See "Taq Colony PCR to check knock-ins/knock-outs" procedure page from CHF Lab Binder). The program used was a "Taq Col" program, utilizing 0.125µL of 5U/µL SibEnzyme Taq DNA polymerase per reaction. The final reaction volume for this PCR was 12.5µL. Forward primers were designed as 20bp oligonucleotides that anneal to a section upstream of where the forward primer used to amplify the cassette would bind (see appendix Table A.3). This ensured the primer annealed outside of the knockout cassette, while reverse checking primers were designed as 20bp oligonucleotides annealing within the selective marker of the cassette (see appendix Table A.4). Results were visualized on an ethidium bromide stained, 1.5% agarose gel run at 95V for about 1 hour.

Tract-Length PCRs and Stability Assays

In order to score each protein or histone lysine residue for its contribution to repeat maintenance, mutant strains were placed in a stability assay. The assay involves 6 to 8 cell divisions of the cell, allowing for induction of expansions and contractions. An overview of this assay, and a diagram of YAC CF1 as a template for Tract PCR, is given in Figure 9.

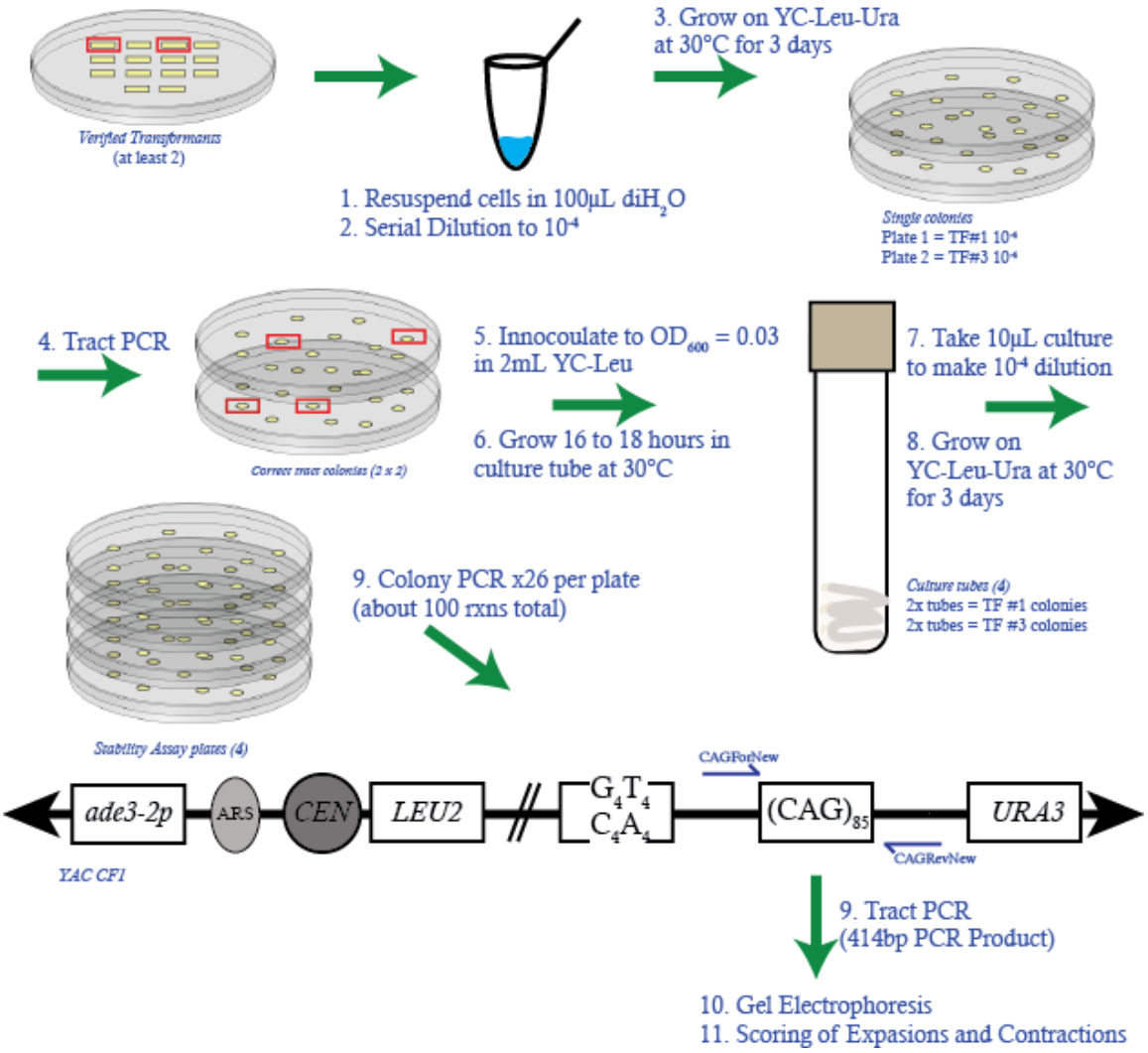

Figure 9. Experimental design of stability assays
Verified mutant transformants were verified for correct $(CAG)_{85}$ tract length, grown for 6 to 8 generations to allow for genomic instability, then plated for single colonies. A second round of Tract PCRs could then be used to quantify the expansion and contraction frequency.

1. Verification of Tract-Lengths in Single Colony Isolates

The tract-length of mutant strains had to be verified for the correct $(CAG)_{85}$ size before beginning stability assays. After verification of correct transformant cassette integration, two to three separate transformant isolates were plated for single colonies to verify the correct CAG-tract length. A small amount of cells was picked using a sterile pipette tip and resuspended in

100µL diH_2O. Serial dilutions to of this suspension were made to a 10^{-4} concentration and plated onto YC-Leu-Ura agar plates. The cells were then grown at 30°C for 2-3 days.

Single colonies grown on these plates were then tested for correct CAG-tract length using a colony PCR (See "Colony PCR to amplify CAG Tract on YAC CF1 with IDPolTaq DNA Polymerase (ID Labs) Kit" page in CHF lab binder). Primers used in this reaction (CAGForNew and CAGForRev) were designed to anneal upstream and downstream of the CAG tract on the YAC. PCR products were run on an ethidium bromide stained, 2% MetaPhor agarose gel at 80V for 1 hour and 30 minutes and visualized using UV radiation. The $(CAG)_{85}$ tract for strains used in this paper, the correct tract-length was indicated by a PCR product about 414bp in length.

2. Stability Assay Cultures and PCR Reactions

Colonies with the correct $(CAG)_{85}$ tract length were then set up for stability assay cultures. In most cases, two colonies from two separate transformant isolates were used as starting cultures (four cultures in total). Cultures were set up by inoculating colonies in 2mL of YC-Leu media to an initial OD_{600} of 0.03 and grown at 30°C in a roller drum for 6 to 8 generations (usually between 16 and 18 hours). This growth period allowed for the possibility of the CAG-tract to expand or contract during replication phases. Growth for 6 to 8 complete generations was checked by measuring for a final OD_{600} value between 2.0 and 5.0. Once sufficient growth had occurred, 10µL of the culture was added to 90µL diH_2O and serial dilutions were made to 100µL of a 10^{-4} dilution factor. This dilution was then plated on YC-Leu-Ura and grown at 30°C for 2-3 days.

Approximately 26 colonies from each stability plate were then used for tract PCR, yielding about 100 reactions total per mutant. Tract PCRs were performed as described above

(See "Colony PCR to amplify CAG Tract on YAC CF1 with IDPolTaq DNA Polymerase (ID Labs) Kit" in CHF lab binder). Gel pictures were saved in digital format to be used for scoring of potential expansions and contractions.

3. Scoring of Expansions and Contractions

Successful reaction sets were scored using Adobe Photoshop (performed by Nealia House). A curved line was drawn corresponding to the normal migration pattern of a $(CAG)_{85}$ PCR product through the gel. Bands that were judged to be clearly above the correct $(CAG)_{85}$ tract length, 414bp, were scored as expansions, while those below that size were scored as contractions; bands on the line were termed unchanged, and the presence of no band indicated a failed reaction and was not counted. For each gel photo, the total number of reactions, expansions, and contractions were recorded. The percent of expansions and contractions out of the total number of reactions was calculated. The percent fold over wild-type expansions and contractions was also calculated. The significance of any increase over wild-type was quantified using Fisher's exact test; p-values below 0.05 were considered significantly different, while a higher degree of significance was labeled to numbers with p-values below 0.01.

Other Procedures

Kar-Cross to Introduce YAC CF1

For the *H2A-N*Δ strain, a kar-cross needed to be performed to introduce the YAC for stability assays. The parent strain, CFY1328, was strain background FY406, containing an endogenous plasmid with an *HTA1-HTB1* insert marked by *URA3*. Additionally, the endogenous *HTA1* and *HTB1* genes were knocked out, thus leaving the only copy of the genes on the plasmid.

Plasmid shuffle was first performed on this strain using a *HIS3*-marked plasmid with a *HTB1-hta1-N*Δ insert (CF plasmid #456). Transformants of this reaction were re-patched onto YC-His and then FOA-Leu plates. The patch onto YC-His ensured that transformants indeed contained the *HIS3*-marked plasmid. The second patch growth on FOA-Leu ensured that these transformants had truly lost the *URA3*-marked plasmid endogenous to parent strain CFY1328.

The first step in the kar-cross was to induce a mutation in the *CAN1* gene of the H2A-NΔ strain. The *CAN1* gene codes for arginine permease, and mutation to the gene confers resistance to the drug canavanine (can^r). This mutation is recessive, therefore allowing for selection against diploid cells resulting from mating. H2A-NΔ was grown overnight at 30°C in 2mL of YEPD. From the culture, 10μL was plated on YC-Arg+CAN and grown for an additional 2 days at 30°C.

The mating step of the kar-cross relies on the mutant *kar1-1* allele in the donor (YAC-containing) strain. The *kar1-1* allele is deficient in karyogamy, meaning two mating cells cannot fully fuse their nuclei, which allows for chromosomal transfer between the two cells without full diploid fusion. In conjunction with the induction of canavanine resistance in the recipient strain, haploid cells containing a YAC can be selected for by dropping out Leu and Ura in media (two auxotrophic markers on the YAC). An additional dropout of Trp was used, since the recipient H2A-NΔ was Trp+. A summary of genotype information of strains used in the mating cross can be found in Table 6.

Table 6. Genotypes of two strains used in kar-cross experiment
Shows the genetic information of the donor kar1-1 strain and recipient H2A-NΔ used in this kar-cross experiment. The use of YC-Leu-Ura-Trp-Arg+CAN plates was determined from these genotypes. This selection ensured the presence of the YAC as well as a selection against diploid cells.

Strain Name (Number)	*H2A-N*Δ, No YAC (CFY3178)	*kar1-1* CAG-85 (#1564)
Mating Type	Mat a	Mat α
Genotype	*LEU2, TRP1, ura3-52, lys2*Δ*, his3*Δ*200,* can^R plasmid = *HIS3*	*kar1-1, ADE2, trp1-289, ura3-52, leu2-3* YAC = *URA3, LEU2, ade3-2p*

To carry out the kar-cross itself, a small amount of *H2A-N*Δ can^R and *kar1-1* cells were resuspended and mixed in 20μL diH_2O. This aliquot was then spotted on a YEPD plate and grown at 30°C for 4 hours. Using a sterile woodstick, the patch was scraped completely and resuspended in 200μL diH_2O. A 1:10 dilution was also made, and both the original suspension and the dilution were spread on separate YC-Leu-Ura-Trp-Arg+CAN plates. The cells were then grown at 30°C for 3-5 days. Colonies that grew were re-patched onto fresh YC-Leu-Ura-Trp-Arg+CAN plates and grown at 30°C for an additional 2 days.

Re-patched strains on YC-Leu-Ura-Trp-Arg+CAN were further verified for successful YAC transfer by performing tract PCR as described above PCR. Strains with the correct tract-length were considered successful kar-crosses, and two such transformants were saved as glycerol and used for subsequent stability assay analysis.

Results

1. Rsc1, Rsc2, and Bdf1 maintain repeat stability in same pathway as Esa1

The purpose of these experiments was to study specific bromodomain-containing chromatin remodelers' contribution to CAG-repeat maintenance. To do this, candidate genes were deleted in the yeast genome, and CAG instability evaluated in the deletion strain compared to the wild-type (WT). In order to see if these remodelers were epistatic with the HAT activity of NuA4 (and thus, likely recruited by acetylation of H4-K12 or H4-K16), or the HDAC activities of Hst1, Hos2, or Sir2, remodeler knockouts were made in NuA4-catalytically dead and HDAC triple knockout backgrounds, respectively.

Using the two-step gene replacement technique, remodeler deletion strains were constructed in wild-type (CFY810), *esa1-1851* (CFY2050) and *hst1*Δ*hos2*Δ*sir2*Δ (CFY2656) BY4705, $(CAG)_{85}$ backgrounds to be used for stability assays. An example of successful knockout cassette PCR reactions for *snf2*Δ*::TRP1* and *snf2*Δ*::KanMX6* fragments, visualized by gel electrophoresis, are shown in Figure 10. Verification of successful integration of the knockout cassette carried out by TaqCol Verification PCR was also successful for these strains. An example of the knockout verification reaction for *snf2*Δ*::TRP1* is shown in Figure 11.

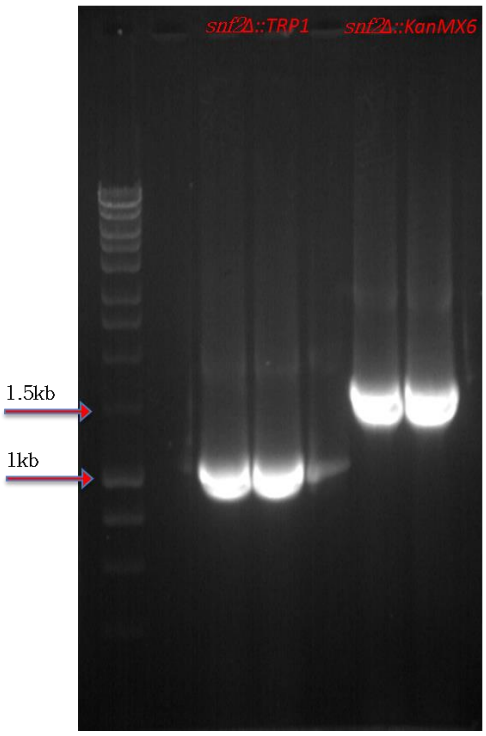

Figure 10. Knockout Cassette Construction for *snf2*Δ*::TRP1* and *snf2*Δ*::KanMX6* Fragments

Using a plasmid-based template, knockout cassettes for the *SNF2* gene were constructed using two different markers. Lanes 2 and 3 show PCR product for the *snf2*Δ*::TRP1* cassette, while lanes 5 and 6 show PCR product for the *snf2*Δ*::KanMX6* cassette. Correct PCR amplification is confirmed by their proximity to 1kb and 1.5kb markers, respectively.

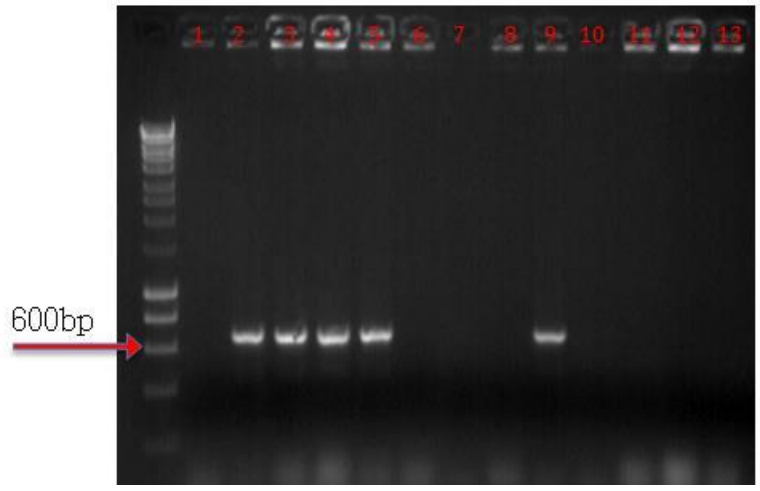

Figure 11. Verification PCR of *snf2*Δ*::TRP1* Transformants

Colony PCR was performed to confirm the integration of the knockout cassette at the gene locus of interest, which for this gel photo, is for the *SNF2* locus. Primers used in this reaction were Snf2 For (CF primer #1159) and 3'Trpverif (CF primer #140). A PCR product of 636bp indicates a correct transformant. For this mutant, transformants 3 and 5 were saved and used for subsequent stability analysis, and saved as strains CFY3086 and CFY3087, respectively.

Tract-lengths of successful transformants were verified using the previously described Tract-Length PCR method. Transformants were plated for single colnoies on YC-Leu-Ura media until sufficiently sized to perform a colony PCR. An example of a successful tract-length PCR for *snf2*Δ $(CAG)_{85}$ strains is shown in Figure 12.

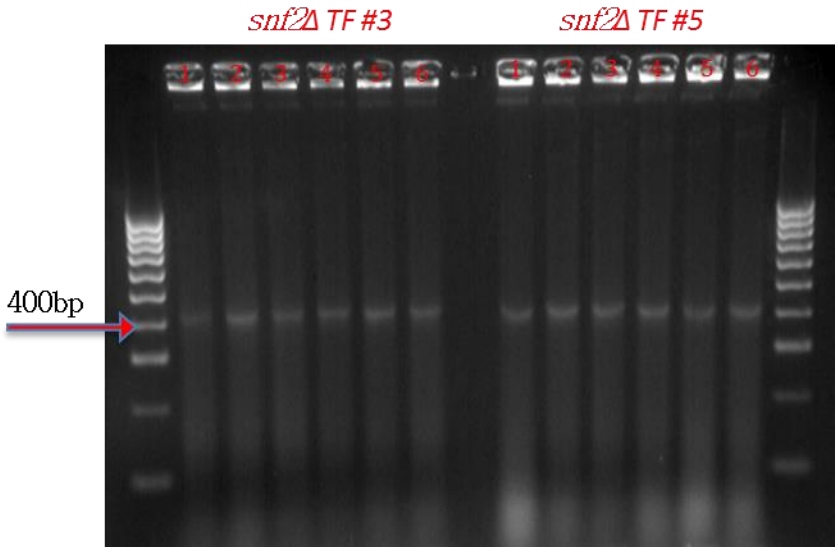

Figure 12. Verification of $(CAG)_{85}$ tract length in *snf2*Δ mutants
Tract PCR was performed on single colony isolates of the *snf2*Δ transformants. Colonies with the correct $(CAG)_{85}$ tract length are indicated by a 414bp PCR product. For stability assays, two colonies from each transformant were used. In the photo above, the four colonies used were colonies 1 and 2 from transformant number 3 (CFY3086), and colonies 2 and 3 from transformant number 5 (CFY3087).

Stability assays of successful transformants with the correct $(CAG)_{85}$ tract were carried out using the methods previously described. Instability data for single remodeler knockouts are given in Figure 13. A summary of raw stability data can be found in appendix Table C.1.

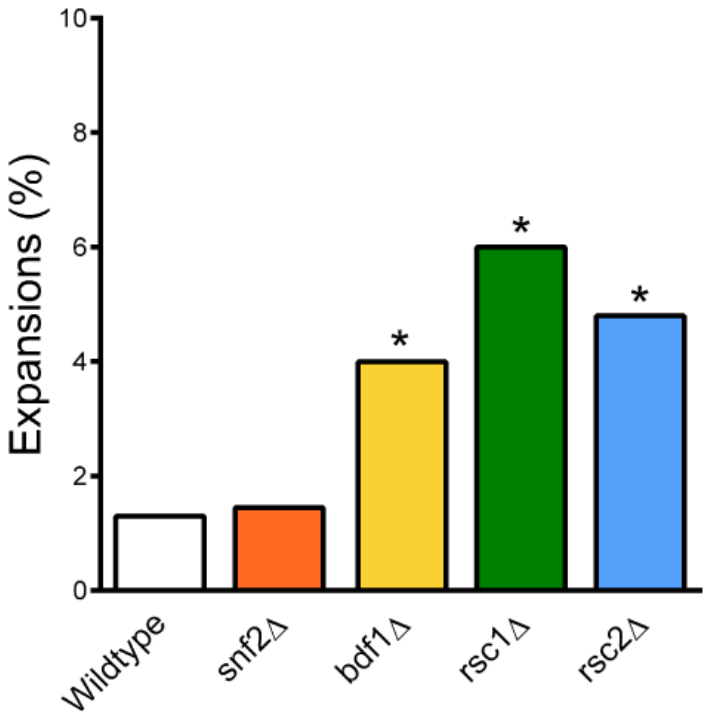

Figure 13. CAG-repeat maintenance by bromodomain-containing chromatin remodelers
Instability of bromodomain-containing single remodeler knockouts was quantified. Among the remodelers, Bdf1, Rsc1, and Rsc2 showed a significant increase in expansion frequency over wildtype. The *rsc1*Δ and *rsc2*Δ strains were constructed by Nealia House; stability assays for *bdf1*Δ, *rsc1*Δ, and *rsc2*Δ were performed by Nealia House.

In the single knockout remodeler mutants, significantly increased expansion frequencies were observed in Bdf1, Rsc1, and Rsc2, but not Snf2. This means Rsc1, Rsc2, and Bdf1 contribute to CAG-repeat stability. If the remodelers act in the same pathway as Esa1, the knockout in the *esa1-1851* background would show the same phenotype as *esa1-1851*. Otherwise, an increased or additive phenotype would be observed, since two separate repair pathways would be inhibited. The *esa1-1851 bdf1*Δ, *esa1-1851 rsc1*Δ, and *esa1-1851 rsc2*Δ all showed similar expansion phenotypes (see appendix Figure C.1), suggesting that all three proteins are epistatic with Esa1, e.g. working in the same pathway. By extension, this could mean the remodeler complexes SWR1 (of which Bdf1 is a subunit) or either isoform of RSC is recruited for repair of the CAG repeat.

Prior lab data indicated sister chromatid recombination (SCR) repair happening at the CAG repeat, and since expansions in the esa1 mutant were dependent on Rad52 and Rad57, it was hypothesized that they might be occurring during SCR. Assays performed using a published assay (Mozlin et al., 2008) showed a decrease in spontaneous and MMS-induced sister chromatid recombination rates for both *rad5*Δ and *esa1-1851* strains, implying that both proteins are involved in error-free sister chromatid recombination (N House, CF Freudenreich, unpublished data). Therefore the roles of Rsc1, Rsc2 and Bdf1 in spontaneous SCR were determined, to see if they were similar to Esa1 (appendix Figures D.2 and D.3). Suppression of SCR was observed in the absence of Rsc1, Rsc2, and Bdf1, suggesting that these proteins are required for SCR. Upon addition of MMS, only *rsc2*Δ and *bdf1*Δ strains displayed a suppression of recombination rates, similar to the *esa1-1851* mutant. Suppression of SCR in the presence of MMS indicates contribution to gap-induced SCR, whereas lack of suppression could indicate that this protein acts in a different pathway, or repairs a different kind of damage, such as a DSB. Therefore, Rsc1 likely acts in a later stage of repair, such as DSBR, consistent with previous findings by Chambers et al. (2012).

Similar expansion frequencies between the *hst1*Δ*hos2*Δ*sir2*Δ strain and remodeler knockouts made in the same triple HDAC mutant would indicate that these proteins are epistatic with one another. This pattern was shown in the Bdf1 and Rsc2 proteins, but a suppression of expansion frequency is seen in the *hst1*Δ*hos2*Δ*sir2*Δ*rsc1*Δ mutant (unpublished). Additionally, ChIP analysis shows a signal for Rsc1 at a later time point than the Rsc2 signal. The Rsc2 signal peaks at 20 min. into S phase, similar to that of H4-K16ac as shown by ChIP (NH, JY and CHF, data not shown). Taken with the SCR data, this suggests that the two isoforms of RSC contribute to CAG repeat maintenance differentially; the Rsc2 isoform of RSC is likely recruited

to the repeat earlier for gap-induced SCR, whereas conversion of gaps into DSBs at later time points of damage would recruit the Rsc1 isoform of RSC to the repeat for repair in a different pathway. Further experimentation is required to directly test these mechanisms.

2. Htz1 and Swr1 do not contribute to CAG-repeat stability

The purpose of these experiments was to show if the deposition of Htz1 by the SWR1 complex (catalytic subunit Swr1) was required to maintain CAG repeat stability. The previous section of results described that the bromodomain-containing proteins Rsc1, Rsc2, and Bdf1 are all involved in CAG repeat maintenance. This implies that two possible remodeling complexes could be acting in prevention of CAG-repeats: the SWR1 or RSC complex.

The Htz1 protein, also known as H2A.Z, is exchanged for H2A in nucleosomes during repair of DSBs by the Swr1 chromatin remodeler (Seeber et al. 2013). Bdf1 is a known subunit of the SWR1 remodeler complex, and our data indicates that Bdf1 plays a role in repeat stability (Fig. 13; Table C.1; Figure C.1). Its role was further characterized as acting independently or within the SWR1 complex by determining if a *swr1*Δ or *htz1*Δ knockout had the same phenotype as the *bdf1*Δ deletion. If the SWR1 complex contributes to CAG repeat maintenance through the recruitment of Bdf1 to acetylated histones, then the Swr1 deletion would show the same expansion phenotype as the Bdf1 deletion. Similarly, if the action of SWR1 at the repeat involves exchange of H2A and Htz1 for repeat maintenance, the Htz1 deletion would also show the same phenotype as the Bdf1 deletion.

Construction of the *htz1*Δ and *swr1*Δ mutant strains was carried out in a wild-type BY4705 $(CAG)_{85}$ background, as previously described. Compared to wild-type expansion frequency, deletion of Swr1 and Htz1 did not lead to an increase in expansion frequency, indicating that neither the Swr1 remodeling protein, nor the Htz1 histone variant protein likely

play a role in maintaining repeat stability through the action of the SWR1 remodeling complex (see Figure 14). This result suggests that the Bdf1 subunit acts independently of the SWR1 complex to maintain repeat stability. Bdf1 is not actually required for SWR1 complex integrity or histone exchange activity (Wu et al, 2009), and has several other functions in the cell. This observation is discussed later in the Discussion section.

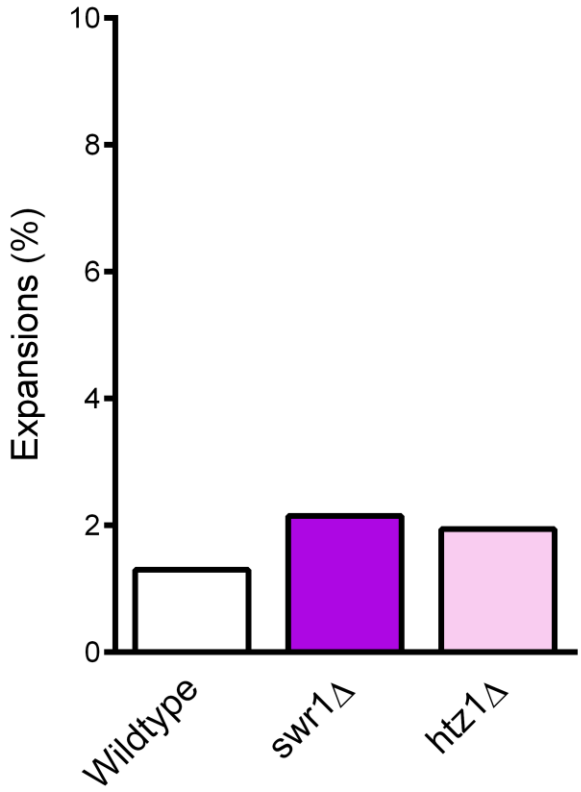

Figure 14. The remodeling protein Swr1 and histone variant Htz1 do not significantly contribute to repeat stability
Compared to wild-type expansion frequency, the *swr1*Δ and *htz1*Δ mutants did not show an increased expansion phenotype. This indicates that the deposition of H2A.Z (Htz1p) by the SWR1 complex is not involved in maintaining CAG repeats.

3. Acetylation of histone H2A does not contribute to repeat stability

In order to confirm that H4 is the relevant target for acetylation by NuA4 (see Figure 5C), stability data for the H2A protein was collected. A strain containing a deletion of the H2A N-terminal tail was constructed to see if this deletion would lead to an increase in CAG instability. Previous data found that both histone H3 (see Figure 5C) and histone variant Htz1 (see Figure 14) do not contribute to CAG-repeat maintenance. However, Esa1 targets lysine residue 7 of histone H2A *in vivo* (Millar and Grunstein 2006), and thus, Esa1 acetylation of the H2A N terminus could play a role in maintaining CAG repeats.

The H2A-*N*Δ strain was constructed in two transformation steps. First, a strain containing single copies of *HTA1* and *HTB1* on a plasmid (CFY1328) was plasmid shuffled with a plasmid containing the genes *HTB1* and *hta1*Δ*5-21* (N-terminal tail delete). Second, a kar- cross was performed to introduce the $(CAG)_{85}$ YAC into the strain.

Stability assays were performed and an expansion frequency of 1.61% (p-value = 1) was calculated. Compared to wild-type expansion frequency, this is not a significant increase in expansion rate (see Figure 15). Thus, the N-terminal tail of histone H2A likely does not play a significant role in maintaining repeat stability. This finding further supports that NuA4 specifically targets H4 for repair of CAG repeats.

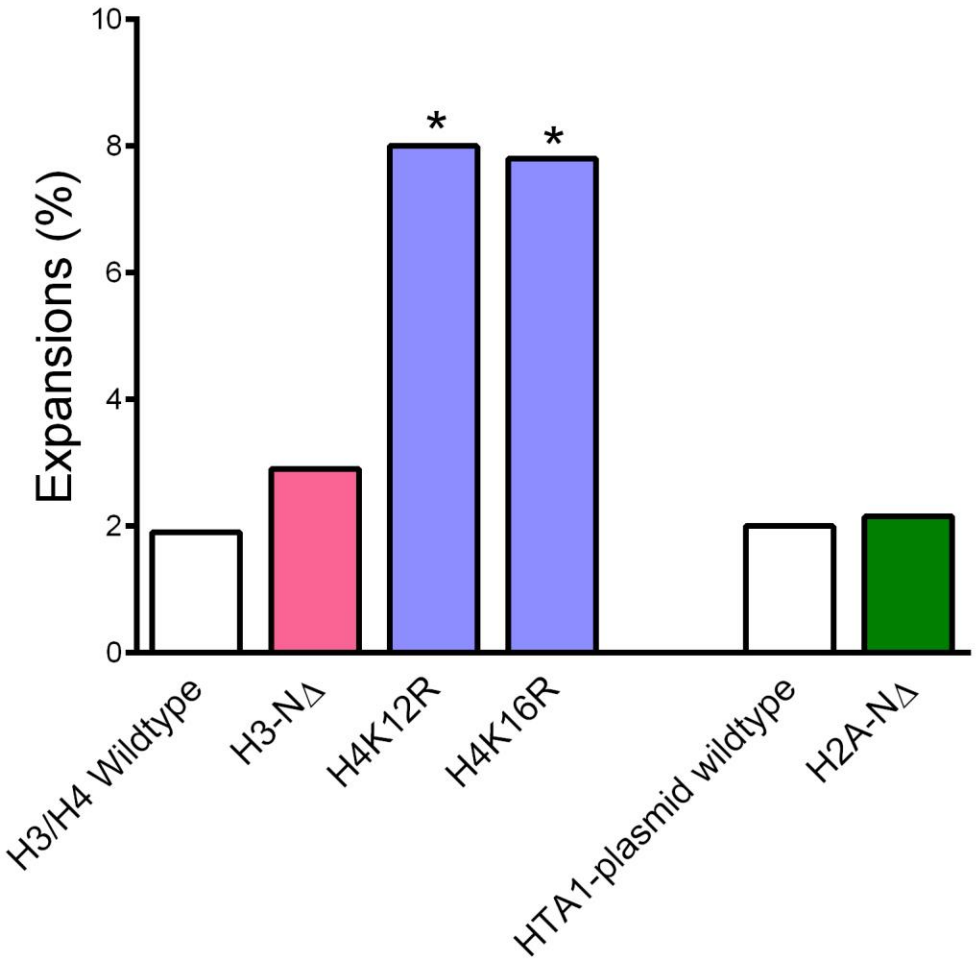

Figure 15. Acetylation of the H2A N-terminal tail does not contribute to repeat stability
While loss of acetylation in H4-K12R and H4-K16R (blue bars) leads to a significant increase in repeat expansions, the loss of acetylation on the H2A N-terminal tail does not lead to an increased expansion frequency compared to wildtype (white bars). The HTA1-plasmid wildtype strain is included as an added control to quantify baseline levels of expansion frequencies in these strains. Stability assays for H3/H4 wildtype performed by Jiahui Yang; stability assays for H3-NΔ, H4-K12R, H4-K16R and HTA1-plasmid strains performed by Nealia House.

4. Deacetylation of H4 lysine residues 5, 8, and 12 is important for CAG repeat maintenance

In order to further support the idea that deacetylation on the H4 N-terminal tail is important in contributing to CAG repeat stability, a strain was constructed with H4 lysine residues 5, 8, and 12 substituted for glutamine. Glutamine (Q) mimics the structure and charge state of acetyl-lysine, and thus mimics a constitutive H4 acetylation state. The mimicked

acetylation state provided by a lysine to glutamine (K to Q) mutation would not result in a significant increase in expansions. This is different than the previously described lysine to arginine (K to R) mutations, where loss of acetylation would presumably lead to a full increase in expansions. Previous data in the lab showed that the expansion frequency of a H4-K16Q mutant had an elevated expansion phenotype, indicating that deacetylation of this residue was important for CAG repeat maintenance, but not statistically significant. The H4-K5,8,12Q mutant was constructed to assess whether or not the deacetylation of these lysine residues 5 would contribute to CAG repeat stability.

The H4-K5,8,12Q mutant was constructed via plasmid shuffle transformation into strain CFY2757 using plasmid (CF plasmid #470 , courtesy of Pillus lab). Transformants were verified by phenotype by re-patching on YC-Leu-Ura-Trp plates, to select for the new plasmid containing the Trp1 marker, and replica-plated onto YC-Met-Cys plates, to confirm the original *MET15* plasmid in strain CFY2757 was lost.

Compared to wildtype, both H4-K16Q and H4-K5,8,12Q mutants showed an elevated repeat expansion frequency (see Figure 16). The elevated expansion rate indicates that a mimic constitutively acetylated H4-tail can induce expansions, and that removal of the acetyl groups by HDACs at H4 residues 5, 8, 12, and 16 is important in repeat stability maintenance. This data provides independent confirmation of the conclusion based on the HDAC mutants that deacetylation of the histone H4 N-terminus is important for preventing CAG expansions.

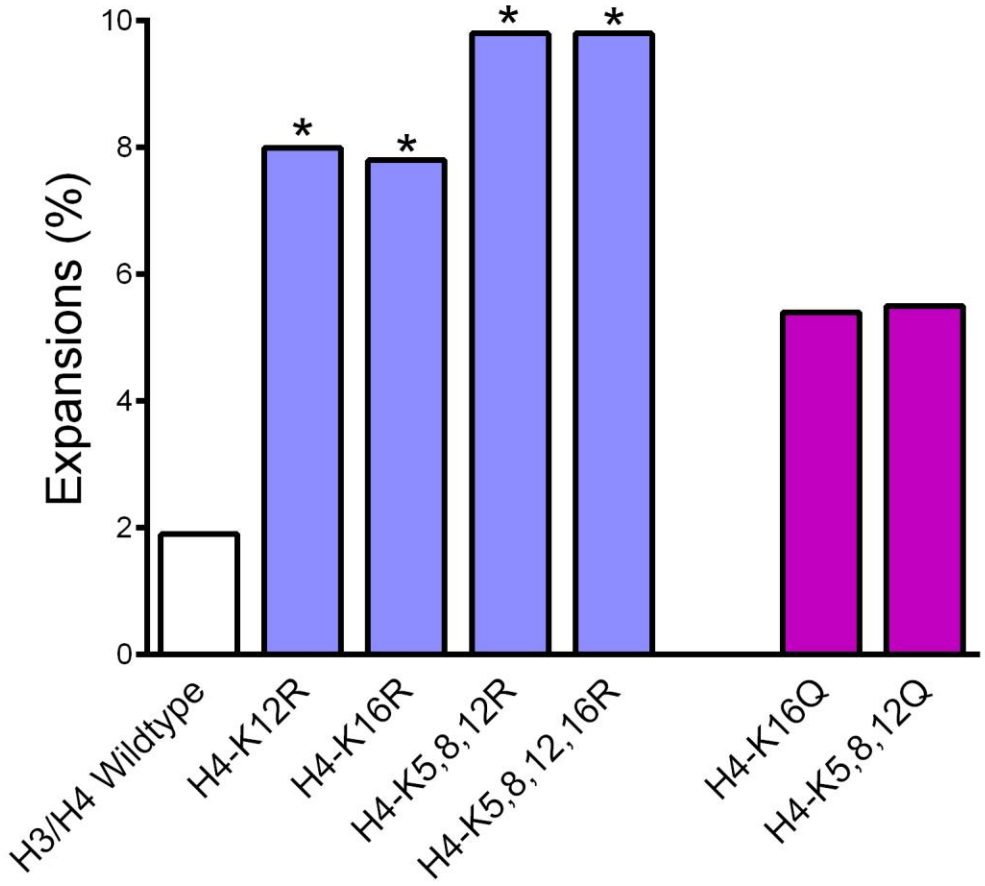

Figure 16. Deacetylation of H4 lysine residues 5, 8, and 12 is important for repeat maintenance

While the acetylation events of H4-K12 and H4-K16 are shown to contribute to repeat stability (blue bars), the contribution caused by deacetylation of specific H4 residues was also quantified in the acetyl-mimic H4-K16Q and H4-K5,8,12Q strains. Data above indicates that deacetylation of residues 5, 8, 12, and 16 is important in maintaining repeat stability, but perhaps not to the same extent as the acetylation of these residues. Stability assays for the H3/H4 wildtype strain were performed by Jiahui Yang; stability assays for H4-K12R, H4-K16R, H4-K5,8,12R, H4-K5,8,12,16R, and H4-K16Q strains were performed by Nealia House.

5. Yng2 contributes to repeat stability maintenance and SCR

The purpose of this experiment was to further support the role of NuA4 in CAG repeat maintenance. More specifically, this experiment was carried out to see if the Yng2 subunit deletion showed a similar expansion phenotype and SCR rate to the *esa1-1851* mutant. Yng2 and Esa1 are both part of the NuA4 complex, and Yng2 is required for positioning of Esa1 to lysine residues (Chittuluru et al. 2011) and thus has an indirect role on acetylation, specifically for histone H4 (Choy and Kron 2002). Together, these experiments further tested the hypothesis that the HAT activity of the NuA4 complex is required for gap-induced, spontaneous SCR at the CAG repeat.

Construction of *yng2*Δ mutant strains was carried out in both a wild-type BY4705 $(CAG)_{85}$ background, to be used for stability assays. The *yng2*Δ mutant showed a statistically elevated expansion frequency compared to wild-type expansion frequency, indistinguishable from previous data for *esa1-1851* expansions (Figure 17). Thus, the Yng2 protein plays a role in maintaining repeat stability, strengthening the conclusion that NuA4 acetylation is required for prevention of CAG-repeat expansions, since the findings of Chittuluru et al. (2011) and Choy and Kron (2002) showed that Yng2 is essential for NuA4 complex integrity.

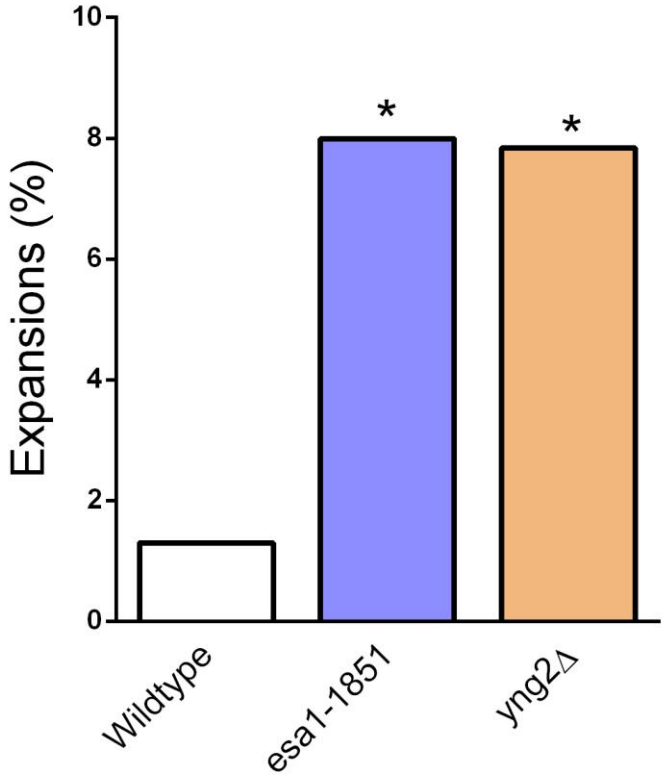

Figure 17. Yng2 contributes to maintenance of repeat stability to the same level as Esa1
The *yng2*Δ mutant displayed a similar expansion phenotype to the *esa1-1851* mutant, and both were significantly increased over wild-type expansion frequency. This data indicates that both of these subunits, part of the NuA4 acetylation complex, are required for CAG repeat stability.

Construction of the *yng2*Δ SCR strain was carried out in a LSY1892 background, as previously described. SCR assays were performed according to the methods described in Appendix D (see Figure D.1). The *yng2*Δ SCR strain showed a similar suppression of sister chromatid recombination to the previously studied *esa1-1851* SCR strain (see Figure 18). Since both subunits are shown to contribute to SCR, this further supports the hypothesis that an intact NuA4 complex is required for SCR. Additionally, the NuA4 subunits Esa1 and Yng2 are required for spontaneous sister chromatid recombination.

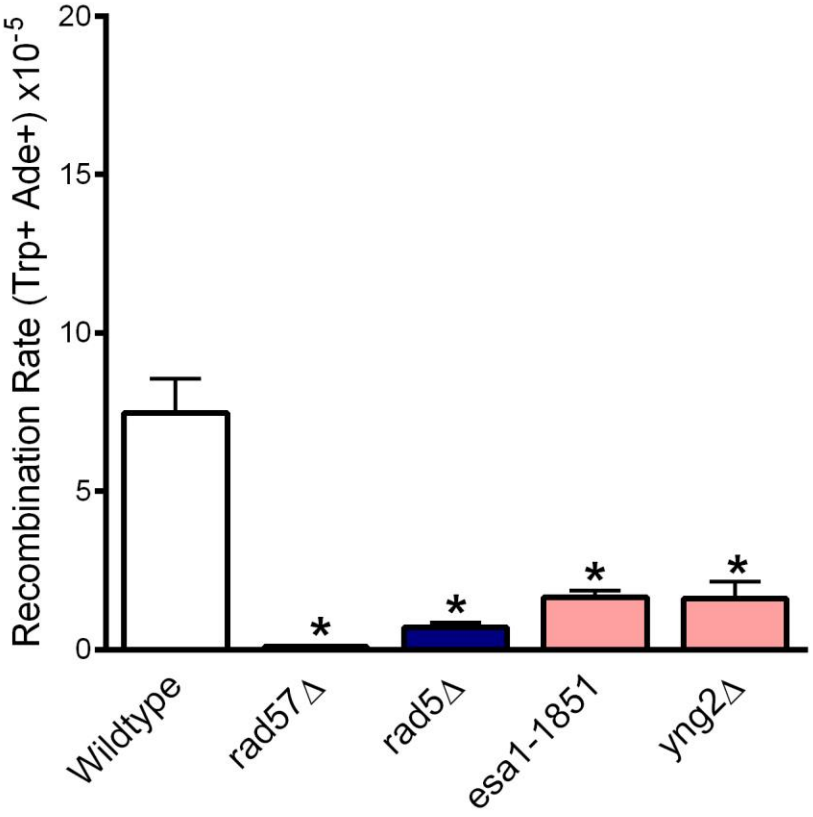

Figure 18. Yng2 contributes to SCR
In the absence of Yng2, sister chromatid recombination was significantly suppressed from wild-type levels. This suppression is somewhat less than the Rad57 and Rad5 deletion strains, which are required for SCR, but similar to the *esa1-1851* mutant strain, indicating that all of these proteins are required for efficient SCR. Raw fluctuation data not included. All SCR assays were performed by Nealia House.

6. Acetylation of H4-K16, and to a lesser extent H4-K12, contributes to sister chromatid recombination

Previous data in the lab indicated that CAG repeats are repaired by gap-induced sister chromatid recombination. However, the specific contribution of acetylation of H4 lysine residues leading to this form of error-free repair had not been directly proven. Since previous data indicated that acetylation of H4-K16, and to a lesser extent, H4-K12, was important in maintaining repeat stability, strains containing mutations in these two residues were constructed in strain backgrounds that can be assayed for unequal sister chromatid exchange. The lysine to

arginine (K to R) mutation inhibits acetylation events, as arginine is not an acetylatable residue. In addition to H4-K12R and H4-K16R SCR strains, an SCR strain containing the H3/H4 wild-type plasmid was constructed for calculation of background sister chromatid recombination rates.

The H4-SCR point mutants were constructed through three separate transformations. First, an *hht2hhf2*Δ*::Kan* fragment was constructed from a genomic template of the H3/H4 wt plasmid yeast strain (CFY2051). This fragment was transformed into the LSY1892 (CFY3104) strain to knockout the *HHT2HHF2* locus on chromosome 14. Transformants were grown on YEPD+G418 and verified using primers listed in Table A.3 and A.4. Next, a plasmid shuffle transformation was carried out to re-introduce the copy 2 histone genes into the transformants, either as the wild-type sequence or with specific point mutations. Finally, an *hht1hhf1*Δ*::His* fragment was constructed from the H3/H4 wt plasmid yeast strain to knockout the *HHT1HHF2* locus on chromosome 2. Transformants were grown and re-patched on YC-Leu-Ura-His plates and verified via colony PCR.

Sister chromatid recombination assays for H4 point mutants were performed as previously described, using Ade+Ura+ revertants (opposed to the Ade+Trp+ revertants used in the *yng2*Δ SCR strain assays). Suppression of SCR was observed in both H4-K12R and H4-K16R strains, but only the H4-K16R strain a significant suppression compared to wild-type levels (see Figure 19).

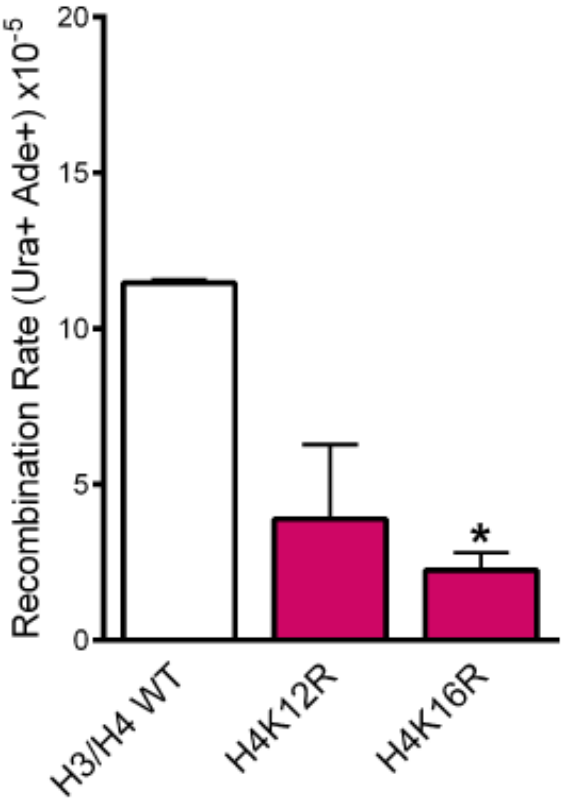

Figure 19. Acetylation of both H4-K12 and H4-K16 contribute to SCR
In the absense of H4-K12 and H4-K16 acetylation, the rate of sister chromatid reocmbination is suppressed. The suppresion in the H4-K16R mutant was statistically significant compared to the H3/H4 plasmid wildtype, indicating that this residue is more important in contributing to SCR. Raw fluctuation data can be found in Appendix Table D.1. All assays performed by Nealia House.

Discussion

The purpose of this project was to better characterize how DNA repair occurs in the context of chromatin at CAG repeats. A specific focus of this study was to investigate the role of chromatin remodeling enzymes in prevention of CAG repeat expansions, and test the model that the purpose of H4K16 acetylation at a CAG repeat is to recruit a remodeler protein to facilitate PRR. Additional studies presented in this thesis explored the specificity of H4 acetylation to CAG repeat maintenance and contribution to SCR. By integrating data from this thesis with prior data collected in our lab, as well as support from the scientific literature, there is strong evidence for a novel model of DNA repair at CAG repeats involving these chromatin remodeling proteins.

Experimental evidence collected for this thesis can be summarized as follows. Stability assays revealed that the bromodomain-containing chromatin remodeling enzymes Rsc1, Rsc2, and Bdf1 maintain CAG repeat stability in epistasis with the NuA4 catalytic subunit Esa1, while the remodeler complex SWR1 and its substrate Htz1, do not significantly impact this stability. Furthermore, the acetylation of the N-terminal tail of histone H2A does not significantly affect CAG repeat stability. The deacetylation of lysine residues 5, 8, and 12 on histone H4 were found to be important in maintaining CAG repeat stability through the studies of an acetyl-mimic. The Yng2 subunit of the NuA4 was also found to contribute to this stability. Finally, the proteins Rsc2, Bdf1, and Yng2, as well as the acetylation of H4-K16, were found to be important in the repair of DNA at CAG repeats via gap-induced SCR.

The model can now be supported and modified as follows. Upon transient forms of endogenous DNA damage, such as nicks, gaps, or hairpins at a CAG repeat, histone H4 is uniquely targeted and acetylated at residue K16 by the NuA4 HAT complex. The catalytic

reaction of acetylating histones requires the action of both the Esa1 HAT subunit, and the Yng2 protein subunit. Acetylation recruits the remodeler protein Rsc2, along with repair proteins involved in the error-free branch of PRR, specifically by sister chromatid recombination. Together, HR-mediated repair occurs via a template switch (Rad5-dependent) mechanism, whereby the RSC complex moves nucleosomes to facilitate progression of the D-loop. Upon completion of repair, HDAC proteins are recruited to deacetylate histones, marking the end of DNA repair. The cascade of repair events results in maintenance of repeat number through high-fidelity repair at the CAG repeat. An updated visual representation of the model, with the Rsc2 and Bdf1 remodeler proteins incorporated, is given in Figure 20.

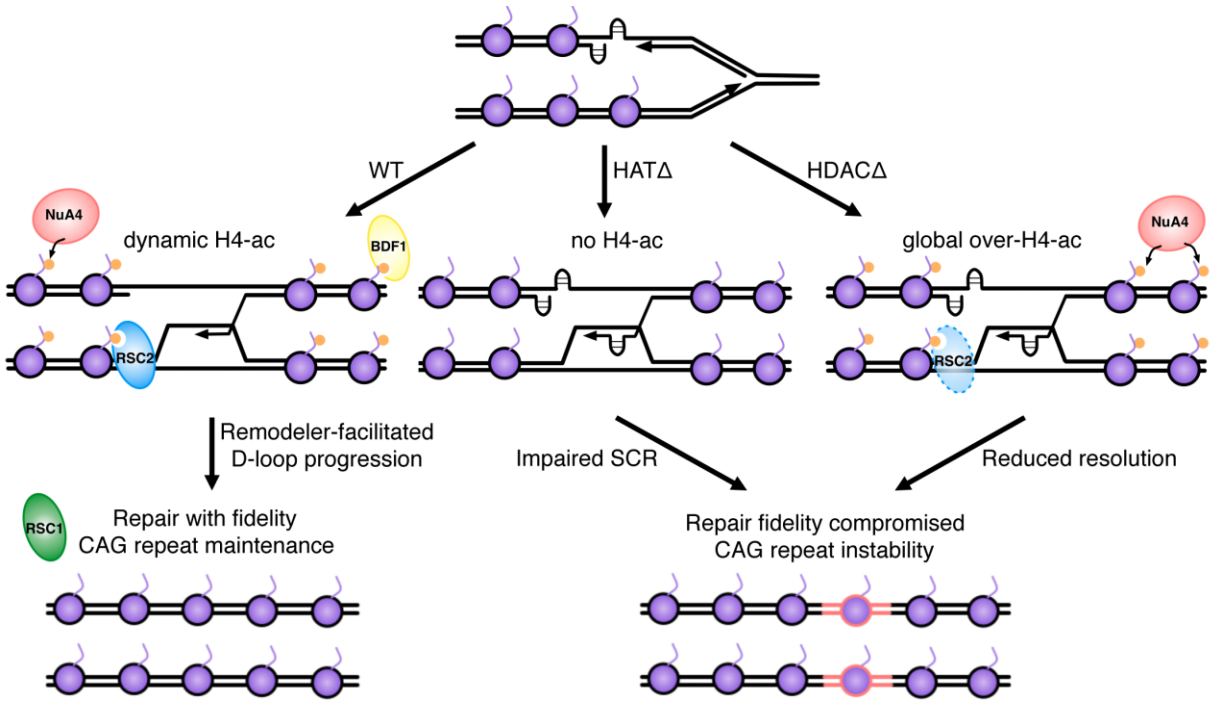

Figure 20. A novel model for dynamic H4 acetylation during post-replicative repair at CAG-repeats

Endogenous forms of DNA damage at the CAG repeat leads to dynamic histone acetylation of histone H4. The acetyl-lysine directly recruits bromodomain-containing remodelers Rsc2 and Bdf1, as well as DNA repair proteins to the site of damage. Upon completion of repair, HDAC proteins remove the acetylation marks, thus maintaining CAG repeat stability. Errors in this pathway, including absence of H4 acetylation or absence of HDAC proteins, leads to impaired SCR or decreased resolution of repair (adapted from House et al., submitted).

To connect back to the original goals of this thesis, the resulting data indicates how H4 acetylation impacts repair fidelity. Indeed, two bromodomain-containing remodeling proteins that affect CAG repeat stability were identified: Rsc2 and Bdf1. The identification of these proteins can be seen as the major contribution of this thesis to the model described previously.

Additional evidence presented in this thesis reinforces the importance of histone H4 acetylation in this model. Previously described results have ruled out the possibility that histones H2A and Htz1, which are relevant targets for acetylation by Esa1 (Millar and Grunstein 2006), contribute to repeat stability. Additional contributions of Yng2 as an essential subunit of NuA4 in this model and the importance of deacetylation of H4-K5, 8, and 12 on repeat stability, were also extensively collected and added to the context of the model.

Finally, the specific contribution of H4 acetylation to sister chromatid recombination was quantified. Deletion of Yng2 led to a significant decrease in sister chromatid recombination, similar to the recombination phenotype of the *esa1-1851* mutant. In the absence of H4 acetylation on residues K12 and K16, rates of sister chromatid recombination were suppressed, more pronounced in the loss of H4-K16 acetylation. These results further indicate the uniquely important acetylation events of histone H4, carried out by the NuA4 complex.

Furthermore, ChIP and SCR assay evidence collected by Nealia House shows that Rsc2 localizes to the repeat 20 minutes after S-phase, a time point corresponding with the H4-K16 acetylation event (see appendix Figure E.2). This reinforces data presented in this thesis with physical evidence for the presence of Rsc2 at the CAG repeat. SCR assays revealed that Rsc2 and Bdf1 are necessary for gap-induced SCR (see appendix Figure D.2). This finding is also in agreement with the involvement of Rsc2 in PRR through PCNA ubiuitination (Chambers et al. 2012), further supporting a DNA repair function of Rsc2 at the CAG repeat.

Future Directions

The remodeler proteins Rsc1 and Rsc2 have not been directly proven to be epistatic to the error-free branch of PRR. In order to test that they truly are part of the same PRR/SCR pathway, double mutants between the RSC subunits and Rad51 or Rad52 can be constructed. Subsequent stability assay analysis of these mutants would reveal more complete evidence that these remodeling proteins promote sister chromatid recombination, since the formation of an invading nucleofilament by Rad51 and later Rad52-mediated strand exchange are both required for PRR. If Rsc1 and Rsc2 are indeed required for PRR, then double mutants of a remodeler and repair protein would show a suppressed expansion phenotype, suggesting that expansions in the absence of Rsc1 or Rsc2 occur through PRR repair pathways (Rad51 and Rad52-mediated). At the time of this writing, *rsc1*Δ*rad51*Δ and *rsc1*Δ*rad52*Δ strains (construction data not shown) have been successfully constructed and verified, with stability analysis forthcoming.

Additional information can be found by constructing Rsc2 and Rsc1 knockouts in H4-K12R and H4-K16R strain backgrounds. Stability data of these mutants would indicate if these mutants are epistatic with the acetylation marks at K12 and K16; epistasis of these two events (Rsc2 remodeling and H4 acetylation) was only indirectly proven due to epistasis with Esa1. Additionally, since both Rsc2 and H4-K16 were found to significantly contribute to SCR, a *rsc2*Δ H4-K16R SCR strain could be constructed and tested with SCR assays to prove that they are truly epistatic with one another and the SCR repair pathway. In addition, the best experiment to test our model would be to determine whether recruitment of Rsc2 to the CAG repeat is abolished in a H4K16 mutant.

Additional tests can be performed to further elucidate the role of Esa1 in relation to acetylation of H4-K12 and H4-K16. A substantial amount of previous data indicates that both the Esa1 HAT activity and H4-K12 and H4-K16 acetylation are important in DNA repair of CAG repeats. However, the acetylation of these two residues was never directly proven to be epistatic with Esa1. To show this, strains containing the *esa1-1851* mutation and the H4-K12R and H4-K16R point mutations can be tested using stability assays. If the acetylation events of these residues are epistatic with Esa1, then there should be no increase in the expansion phenotype, thus supporting the current model.

Since Rsc1 and Rsc2 ChIP data shows they localize to the repeat at different times in S-phase, another experiment that could shed light on this process is constructing Rsc1 and Rsc2 tagged strains in H4-K12R and H4-K16R backgrounds. The physical evidence for their existence at the repeat has been shown by previous ChIP data, and this experiment would be an added experimental data point to further support their presence at the repeat. Since recruitment of these two remodelers is depended upon H4 actylation, the loss of acetylation at H4-K12 and H4-K16 should lead to a loss of signal during this ChIP experiment.

The role of the Rsc2 isoform of RSC remains the best characterized in this model, but the stability data and SCR data still suggest a role of Bdf1, acting independently of the SWR1 remodeling complex. Bdf1 has been shown to tightly bind acetylated histone H4-K12 but is inhibited from binding upon acetylation of H4 K16, acting as a switch between heterochromatic and euchromatic states (Millar et al. 2004). Upon damage, acetylation of K-16 would cause Bdf1 to fall off, as suggested in the "switch" by Millar (2004). For the model, genetic evidence indicates that both H4-K12 and H4-K16 acetylation occur at the repeat. ChIP data reveals that H4-K16 acetylation happens roughly 20 minutes into S-phase, when Rsc2 is recruited (see

Figure E.2), but H4-K12 acetylation was not specifically detected at the repeat. Bdf1 could be tightly binding the acetylated H4-K12 residue, making it harder to detect by ChIP. Alternatively, H4-K12 acetylation may be constitutive, not damage-induced. H4-K12 ChIP in the *bdf1*Δ mutant might distinguish between these two possibilities. However, this experiment would only be useful if Bdf1 is shown, by ChIP, to bind at the CAG repeat.

To see if Bdf1 truly binds at the repeat, strains could be constructed with Bdf1 tagged for ChIP analysis. At present, strains with Bdf1 marked with the TAP-tag have been successfully constructed in $(CAG)_0$ and $(CAG)_{155}$ strain backgrounds (construction data not shown). Additional construction of Bdf1 tagged in a H4-K12R would also allow for a good negative control, if Bdf1 is truly binding H4-K12ac at the CAG repeat. In this strain, the ChIP signal should be lost, which could further shed light on the poorly understood role of Bdf1 at the CAG repeat during repair. Additionally, ChIP experiments for Bdf1 in a H4-K16R background could show if Bdf1 is directly recruited by acetylation of H4-K16, and provide a good experimental comparison to the H4-K12R ChIP data. According to the evidence collected for this project, and in relation to the proposed model, a signal for the Bdf1 protein should be seen sometime before 20 minutes into S-phase. This precedes H4-K16 acetylation, as well as Rsc2 recruitment, and could potentially correspond to H4-K12 acetylation. Further, aprotein peak before 20 minutes would indirectly support the evidence that Bdf1 falls off of the acetylated tail upon H4-K16 acetylation.

A summary of future strains that can be constructed, and what information subsequent stability analysis, SCR analysis, or ChIP analysis could result, is given in Table 7.

Table 7. Future strain constructions, directions of this project

This table outline different strains that can be constructed to further elaborate the novel model of CAG repeat repair. At present, a handful of these strains have been constructed, or are in the process of being constructed, for future analysis.

Strain(s) to be constructed	Relevant analysis	Purpose
*rsc1*Δ*rad51*Δ *rsc1*Δ*rad52*Δ *rsc2*Δ*rad51*Δ *rsc2*Δ*rad52*Δ	Stability assays	Show that Rsc1 and Rsc2 are epistatic with these PRR proteins
*rsc1*Δ H4-K12R *rsc1*Δ H4-K16R *rsc2*Δ H4-K12R *rsc1*Δ H4-K16R	Stability assays	Further support that acetylation of H4-K12 and H4-K16 are epistatic with Rsc1 and Rsc2
*rsc2*Δ H4-K16R SCR	SCR assays	Test if the involvement of Rsc2 in SCR is dependent upon acetylation of H4-K16
esa1-1851 H4-K12R *esa1-1851* H4-K16R	Stability assays	Further support of Esa1 acetylation on H4-K12 and H4-K16 in prevention of CAG repeat expansion
Rsc1-TAP H4-K12R Rsc1-TAP H4-K16R Rsc2-TAP H4-K12R Rsc2-TAP H4-K16R	ChIP	Show if loss of acetylation on these histone residues results in loss of physical interaction of Rsc1 and Rsc2 at the CAG repeat
Bdf1-TAP $(CAG)_0$ Bdf1-TAP $(CAG)_{155}$ Bdf1-TAP $(CAG)_{155}$ H4-K12R Bdf1-TAP $(CAG)_{155}$ H4-K16R	ChIP	See if Bdf1 localizes to the CAG repeat, and if so the timing; see if it is dependent upon H4-K12 or H4-K16 acetylation at the repeat

Appendix A. Primer Information

Table A.1. pFA Primers used in plasmid-template knockout cassette construction
Each 60bp primer contains a conserved 20bp sequence at its 3' end homologous to sequences upstream and downstream of the selectable marker on any pFA plasmid. The other 40bp of the primers correspond to sequences directly upstream and downstream of the ORF of the gene of interest.

Gene Knockout	Primer Name	CF Primer Number	Sequence (5'→3')
RSC1	Rsc1-pFA For	1075	CTAGCTACAAAACAGAGATAAAAAAAATTATATTTCAAG CCGGATCCCCGGGTTAATTAA
	Rsc1-pFA Rev	1076	GCATGAACATATATAGATACATGTGGTGAATTTACATGG GAATTCGAGCTCGTTTAAAC
RSC2	Rsc2-pFA For	1077	AGAACCAGACGAAGCGGAGAATATTCTACATTGACAGT GCCGGATCCCCGGGTTAATTAA
	Rsc2-pFA Rev	1078	GGAAGATATTATGCTGCCATTGCTTTTACAATAAAGGTG AGAATTCGAGCTCGTTTAAAC
BDF1	Bdf1-pFA For	1066	AAAGGCGGTCGAATCTCAACGGCTCTGATAAACGTACGT ACGGATCCCCGGGTTAATTAA
	Bdf1-pFA Rev	1067	TTCTTCTCAGTCGTTGAAGATAATCAAATTCAAAATTCA GGAATTCGAGCTCGTTTAAAC
SNF2	Snf2-pFA For	1068	ACTTTCTGCTATTTTCACGACTTTCGATTAATTATCTGCC CGGATCCCCGGGTTAATTAA
	Snf2-pFA Rev	1069	CGTATAAACGAATAAGTACTTATATTGCTTTAGGAAGGT AGAATTCGAGCTCGTTTAAAC
YNG2	Yng2-pFA For	1290	GGATATGCAAGTTTATATTGGACAACATAACCAATAGAA GCGGATCCCCGGGTTAATTAA
	Yng2-pFA Rev	1291	GTGTAAATGAGGTCATTCAGTCTCAAAAAGGTATTTTTG TGAATTCGAGCTCGTTTAAAC
HTZ1	Htz1-pFA For	1152	AATTTCGCACTATAGCCGCACGTAAAAATAACTTAACAT ACGGATCCCCGGGTTAATTAA
	Htz1-pFA Rev	1153	AGGGAGAATTACGGGAAATGGGAAAGAAAAACTATTCT TCGAATTCGAGCTCGTTTAAAC
RAD54	Rad54-pFA For	1080	AGCTCTATTTCAAGGTACCATATATATTTCCTTATAACTG CGGATCCCCGGGTTAATTAA
	Rad54-pFA Rev	1081	ACTTTTTGTTTTTGTTTTATAAGTACATGTATGTAAGAGA GAATTCGAGCTCGTTTAAAC
FUN30	Fun30-pFA For	1070	TAAACAAGAAAAAGAGAGAAAATACGCTATAGTTGAAA ACCGGATCCCCGGGTTAATTAA
	Fun30-pFA Rev	1071	TCTGCTTATCTATTTACTTTTTTCTATATTTTTATTTATGA ATTCGAGCTCGTTTAAAC

Table A.2. Primers used in genomic DNA template knockout cassette construction
Primers for the desired knockout cassette made from gDNA, as well as location upstream or downstream from the relevant start and stop codons, are listed below.

Desired Cassette	Template gDNA Strain	Primer Name	CF Primer Number	Distance Upstream / Downstream	Sequence (5'→3')
swr1Δ::KanMX6	*swr1Δ::KAN* gDNA (CFY1468)	Swr1 for	1284	178bp	CGTGCAAAAAGGATAGATTT
		Swr1 rev	1285	203bp	ATCACCCGGTAAATAGAAAT
hht1hhf1Δ::His3MX6	H3/H4 wild-type gDNA (CFY2051)	HHF1 rev	419	200bp	CAAGTTCGGTAAGTAGCAGA
		HHT1 rev	415	200bp	TTTCGAGGGTATCGCCAGGA
hht2hhf2Δ::KanMX6	H3/H4 wild-type gDNA (CFY2051)	HHT2 chkdown	1337	235bp	GTAGACAGTGATTACCTTTACG
		HHT2HHF2KOChk	635	300bp	TGGGTTTCTGCGTAAATATT

Table A.3. Forward primers used in mutant verification PCRs
Forward primers were used along with primers listed in Table 9 to check for integration of the knockout cassette at the correct gene locus.

Gene Knockout	Forward Primer Name	Primer Number	Distance Upstream Start Codon	Sequence (5'→3')
RSC1	Rsc1 For	1076	183bp	TTACCCTCTTTCCGTCAATA
RSC2	Rsc2 For	1079	198bp	GCTCTTGCACTTGGTTTATT
BDF1	Bdf1 For	1157	169bp	CGTCGCGAAGTATTTAAACA
SNF2	Snf2 For	1159	86bp	ATAAATCATCGGGAAGGTCA
YNG2	Yng2-292bp-For	1377	292bp	CGCCGTATATTCAGCAAGTA
HTZ1	Htz1-For-chk	1283	299bp	TACTGAATGCATCCATGCTA
hht2hhf2Δ::KanMX6	HHT2ChkDown2-396bpdown	1375	396bp	GCATTTCCGAAGGCCAGGGC
hht1hhf1Δ::His3	HHT1HHF1KOChk	638	245bp	CCACATGGAAAGCCATAAATCTTGC
RAD54	Rad54 For Chk	1155	173bp	AGATCTAACTGAAGCGAAGG
FUN30	Fun30 For	1281	120bp	TAAATCAGTACTGGCGTGTG

Table A.4. Reverse primers used in mutant verification PCRs

Reverse primers were used along with primers listed in Table 8 to check for integration of the knockout cassette at the correct gene locus.

Primer Name	**Primer Number**	**Distance Downstream of Start Codon**	**Sequence (5'→3')**
KanB	15	250bp downstream from start of *KanMX6*	CTGCAGCGAGGAGCCGTAAT
3'Trpverif	140	550bp downstream from *TRP1*	GCTGCACTGAGTAGTATGTTGC
His3RevSK	375	863bp downstream from start of *HIS3*	TTAGATAAATCGACTACGGCAC

Appendix B. *Saccharomyces cerevisiae* mutant strain information

Table B.1. Strains constructed during this thesis study

Strain names and numbers, along with relevant genotype information, is included below. The *esa1-1851* $(CAG)_{155}$ strain was also constructed by a transformation by Nealia House, and confirmed by sequencing by SW.

Strain Name	Strain Number(s)	Strain Background	Parent Strain	Genotype
*bdf1*Δ	CFY3002 CFY3003	BY4705	CFY810	Mat α, ade2Δ::hisG, his3Δ200, leu2Δ0, lys2Δ0, met15Δ0, trp1Δ63, ura3Δ0, bdf1Δ::TRP1; YAC = $(CAG)_{85}$, URA3, LEU2, ade2-3p
*bdf1*Δ *esa1-1851*	CFY2894 CFY2895	BY4705	CFY2050	Mat α, ade2Δ::hisG, his3Δ200, leu2Δ0, lys2Δ0, met15Δ0, trp1Δ63, ura3Δ0, esa1-1851-Kan, bdf1Δ::TRP1; YAC = $(CAG)_{85}$, URA3, LEU2, ade2-3p
*hst1*Δ*hos2*Δ *sir2*Δ *bdf1*Δ	CFY2896 CFY2897	BY4705	CFY2656	Mat α, ade2Δ::hisG, his3Δ200, leu2Δ0, lys2Δ0, met15Δ0, trp1Δ63, ura3Δ0, hst1Δ::HIS, hos2Δ::KAN, sir2Δ::Hph bdf1Δ::TRP1; YAC = $(CAG)_{85}$, URA3, LEU2, ade2-3p
*snf2*Δ	CFY3086 CFY3087	BY4705	CFY810	Mat α, ade2Δ::hisG, his3Δ200, leu2Δ0, lys2Δ0, met15Δ0, trp1Δ63, ura3Δ0, snf2Δ::TRP1; YAC = $(CAG)_{85}$, URA3, LEU2, ade2-3p
*snf2*Δ *esa1-1851*	CFY2898 CFY2899	BY4705	CFY2050	Mat α, ade2Δ::hisG, his3Δ200, leu2Δ0, lys2Δ0, met15Δ0, trp1Δ63, ura3Δ0, esa1-1851-Kan, snf2Δ::TRP1; YAC = $(CAG)_{85}$, URA3, LEU2, ade2-3p
*hst1*Δ*hos2*Δ *sir2*Δ*snf2*Δ	CFY2900 CFY2901	BY4705	CFY2656	Mat α, ade2Δ::hisG, his3Δ200, leu2Δ0, lys2Δ0, met15Δ0, trp1Δ63, ura3Δ0, hst1Δ::HIS, hos2Δ::KAN, sir2Δ::Hph ; YAC = $(CAG)_{85}$, URA3, LEU2, ade2-3p snf2Δ::TRP1
*yng2*Δ	CFY3154	BY4705	CFY810	Mat α, ade2Δ::hisG, his3Δ200, leu2Δ0, lys2Δ0, met15Δ0, trp1Δ63, ura3Δ0, yng2Δ::KanMX6; YAC = $(CAG)_{85}$, URA3, LEU2, ade2-3p
*yng2*Δ SCR	CFY3109 CFY3110	W303	CFY2867	LSY1519-1D; matα, ade2-nde1-::TRP1::ade2-I-Sce1+/aatII-; RAD5+, ade2-1 trp1-1 his3-11,15 can1-100 ura3-1 leu2-3,112, yng2Δ::KanMX6
*htz1*Δ	CFY3088 CFY3089	BY4705	CFY810	Mat α, ade2Δ::hisG, his3Δ200, leu2Δ0, lys2Δ0, met15Δ0, trp1Δ63, ura3Δ0, htz1Δ::KanMX6; YAC = $(CAG)_{85}$, URA3, LEU2, ade2-3p
*swr1*Δ	CFY3107 CFY3108	BY4705	CFY810	Mat α, ade2Δ::hisG, his3Δ200, leu2Δ0, lys2Δ0, met15Δ0, trp1Δ63, ura3Δ0, swr1Δ::KanMX6; YAC = $(CAG)_{85}$, URA3, LEU2, ade2-3p
*H2A-N*Δ	CFY3180 CFY3181	FY406	CFY1328	Mat a, LEU2, TRP1, ura3-52, lys2Δ, his3Δ200; plasmid = H2A-NΔ(5-21) HIS3, ampR, CEN, HTB1; derivative of

				FB639(pT52); from Winston lab; YAC = $CAG)_{85}$, URA3, LEU2, ade3-2p
H4-K5,8,12Q	CFY3288 CFY3289	BY4705	CFY810	Mat α, ade2Δ::hisG, his3Δ200, leu2Δ0, lys2Δ0, met15Δ0, trp1Δ63, ura3Δ0, hht1hhf1Δ::His, hht2hhf2Δ::Kan; CF plasmid #470 (pRS314, TRP1, HHT2, hhf2-K5,8,12Q); YAC = $(CAG)_{85}$, URA3, LEU2, ade2-3p
H3/H4 wildtype SCR	CFY3165 CFY3166	W303	CFY3104	MATα, trp1-1, his3-11,15 can1-100 lue2-3,112 ade2-n-URA3-ade2-a RAD5 hht2hhf2Δ::Kan, hhf1hht1Δ::His3Mx6, with H3/H4 WT pRS314 plasmid (TRP1, CHF#319)
H4-K12R SCR	CFY3167 CFY3168	W303	CFY3104	MATα, trp1-1, his3-11,15 can1-100 lue2-3,112 ade2-n-URA3-ade2-a RAD5 hht2hhf2Δ::Kan, hhf1hht1Δ::His3Mx6, H4-K12R pRS314 plasmid (TRP1, CHF#320)
H4-K16R SCR	CFY3169	W303	CFY3104	MATα, trp1-1, his3-11,15 can1-100 lue2-3,112 ade2-n-URA3-ade2-a RAD5 hht2hhf2Δ::Kan, hhf1hht1Δ::His3Mx6, with H4-K16R pRS314 plasmid (TRP1, CHF#321)
*rad54*Δ	CFY2892 CFY2893	BY4705	CFY810	Mat α, ade2Δ::hisG, his3Δ200, leu2Δ0, lys2Δ0, met15Δ0, trp1Δ63, ura3Δ0, rad54Δ::TRP1; YAC = $(CAG)_{85}$, URA3, LEU2, ade2-3p
*hst1*Δ*hos2*Δ *sir2*Δ*fun30*Δ	CFY2901	BY4705	CFY2656	Mat α, ade2Δ::hisG, his3Δ200, leu2Δ0, lys2Δ0, met15Δ0, trp1Δ63, ura3Δ0, hst1Δ::HIS, hos2Δ::KAN, sir2Δ::Hph fun30Δ::TRP1; YAC = $(CAG)_{85}$, URA3, LEU2, ade2-3p
esa1-1851 $(CAG)_{155}$	CFY3156 CFY3157	BY4705	CFY767	Mat α, ade2Δ::hisG, his3Δ200, leu2Δ0, lys2Δ0, met15Δ0, trp1Δ63, ura3Δ0, esa1-1851-Kan; YAC = $(CAG)_{155}$, URA3, LEU2, ade2-3p

Creation of Yeast Glycerol Stocks

For each strain, two separate transformant isolates with confirmed knockout integration and tract-length were saved as glycerol stocks. Strains were inoculated in 2mL of either YC-Leu media (for YAC-containing strains) or YEPD media (no YAC strains) and grown overnight at 30°C in a roller drum to stationary phase. Cells were resuspended in glycerol (final concentration 15%), vortexed for 1 minute, and stored at -80°C.

Appendix C. Additional Stability Assay Data

Table C.1. Raw stability assay data of strains constructed in this study

Lists the total reactions, expansions, and contractions scored from stability assay analysis. Rates of expansions and contractions were calculated, along with significance compared to wild-type expansion / contraction frequency, using Fisher's exact test. Strains with significantly elevated expansion frequencies ($p < 0.05$) contribute to CAG-repeat maintenance (adapted from House et al., submitted). Assays for *snf2Δ, swr1Δ, htz1Δ, yng2Δ*, H2A-NΔ, and H4-K5,8,12Q strains performed by SW; all other assays performed by Nealia House.

$(CAG)_{85}$ strain	Total reactions	Expansions				Contractions			
		#	%	Fold over wt	p-value to wt	#	%	Fold over wt	p-value to wt
bdf1Δ	202	8	4.0	3.0	0.04	53	26.2	2.4	1.9×10^{-5}
bdf1Δ esa1-1851	103	7	6.8	5.1	7.9×10^{-3}	12	11.6	1.1	0.86
bdf1Δhst1Δ hos2Δsir2Δ	99	7	7.1	5.3	6.6×10^{-3}	14	14.1	1.3	0.47
snf2Δ	96	1	1.5	1.1	1	10	10.4	0.9	1
snf2Δ esa1-1851	104	9	8.7	6.5	1.0×10^{-4}	18	17.3	1.6	0.12
snf2Δhst1Δ hos2Δsir2Δ	103	10	9.7	7.3	3.2×10^{-4}	18	17.5	1.6	0.12
swr1Δ	93	2	2.15	1.61	0.63	15	16.13	1.46	0.21
htz1Δ	103	2	1.94	1.45	0.65	24	23.30	2.11	3.1×10^{-3}
yng2Δ	102	8	7.84	5.8	2.7×10^{-3}	14	13.73	1.24	0.48
H2A-NΔ	93	2	2.15	1.61	1	25	26.88	2.44	0.03
H4-K5,8,12Q	109	6	5.50	4.11	0.17	27	24.77	2.24	0.16
rad54Δ	175	12	6.9	5.1	2.4×10^{-3}	30	17.14	1.55	0.07
fun30Δ hst1Δhos2Δ sir2Δ	100	8	8.0	6.0	2.4×10^{-3}	14	14.00	1.27	0.47

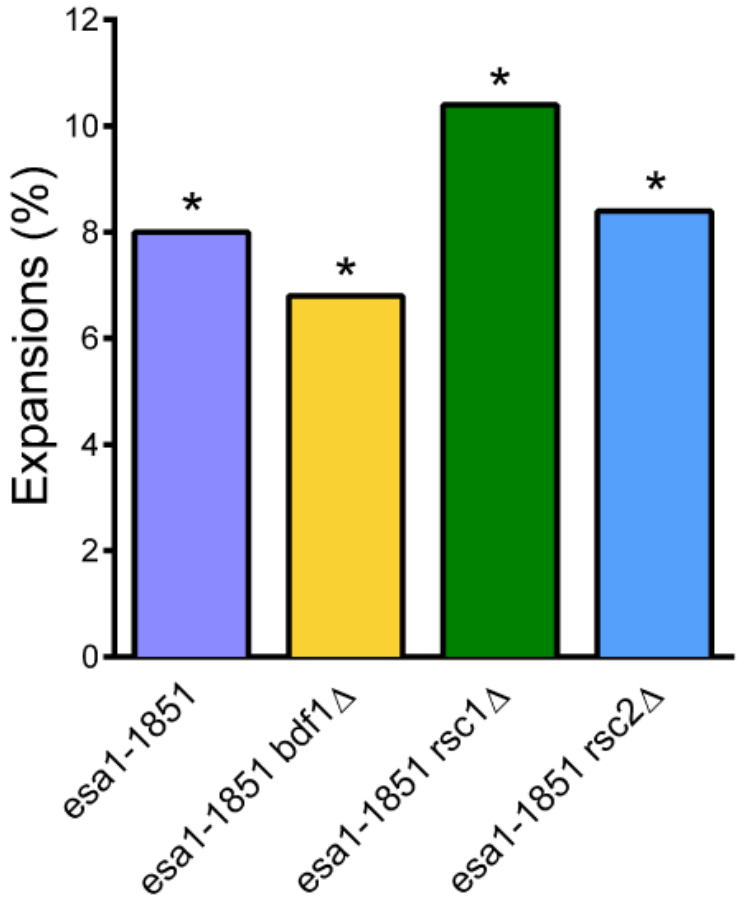

Figure C.1. Bromodomain-Containing Remodelers show Epistasis with Esa1
The remodelers Bdf1, Rsc1, and Rsc2 were found to be epistatic with Esa1 based on similar expansion phenotype. If the remodelers acted in different pathways from Esa1, expansion frequency would be elevated over the frequency of the *esa1-1851* mutant. Stability assays for the *esa1-1851* strain were performed by Jiahui Yang; all other assays performed by Nealia House. (adapted from House et al., submitted).

Appendix D. SCR Assay Information

Sister Chromatid Recombination Assays

In order to assess the rates of sister chromatid recombination, an assay that measures the rate of unequal sister chromatid exchange as a rate of overall SCR was used (Figure D.1). Assays were performed as described (Nealia House, PhD Thesis 2013; modified from Mozlin et al, 2008).

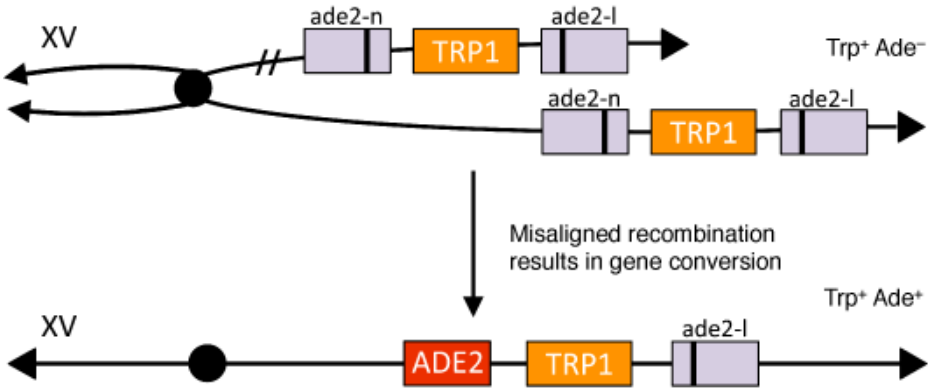

Figure D.1. Representation of Sister Chromatid Recombination assay
This assay measures unequal sister chromatid exchange on a modified chromosome XV. The chromosome contains two separate *ADE2* mutant alleles. The *ade2-n* allele contains a 2bp insertion at an *NdeI* restriction site, while the *ade2-I* allele contains I-SceI cut site insertion, both of which result in frameshift mutations. When unequal sister chromatid recombination occurs at either allele, strains undergo gene conversion from Trp+Ade- to Trp+Ade+. For the LSY1892 background (CFY3104), the same scheme applied, but chromosome XV contained a *URA3* marker instead of *TRP1*, thus revertants were Ura+Ade+ (Figure adapted from Mozlin et al. 2008).

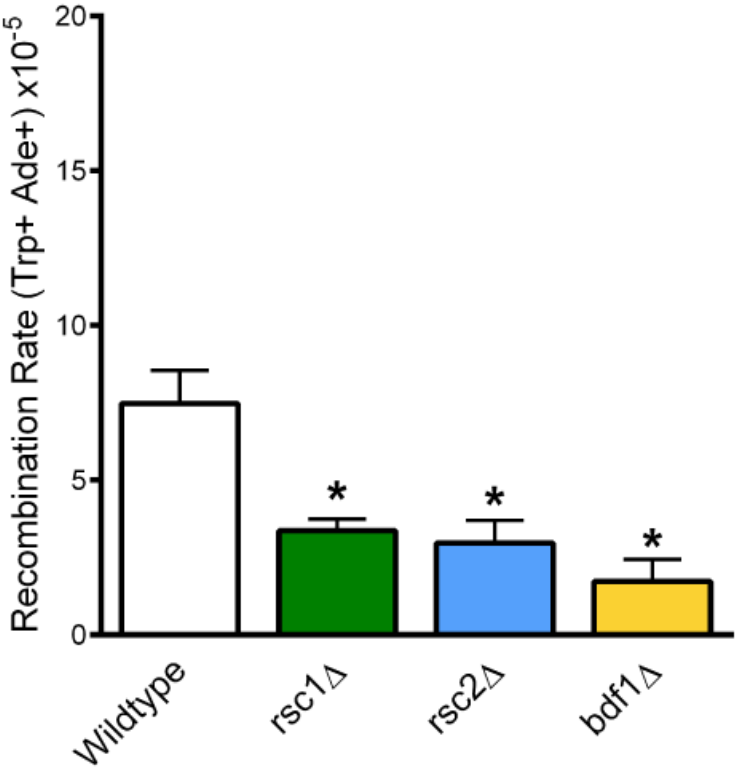

Figure D.2. Rsc1, Rsc2, and Bdf1 are required for spontaneous SCR
Suppression of recombination rate compared to wildtype indicates that protien is required for spontaneous SCR. Absense of the Rsc1, Rsc2, and Bdf1 proteins showed a suppressed recombination phenotype, indicated their requirement for spontaenous SCR. Assays performed by Nealia House (adapted from House et al., submitted).

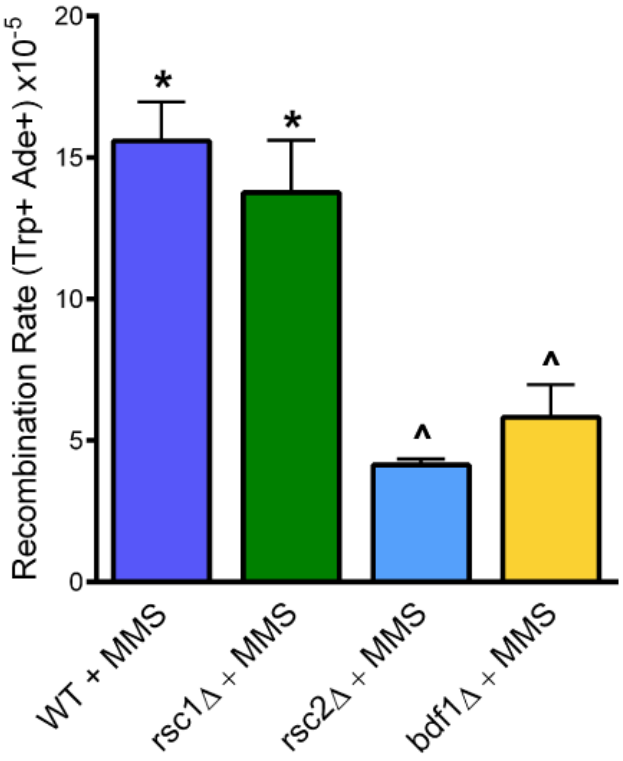

Figure D.3. Bdf1 and Rsc2 are required for gap-induced SCR
Suppression of recombination rate compared to wildtype upon MMS treatment indicates that protien is required for gap-induced SCR. Absense of the Rsc1 protein did not result in suppression of recombination rates, but absense of Bdf1 and Rsc2 did result in significantly suppressed recombination rates, indicating their requirement for gap-induced SCR. Assays performed by Nealia House (adapted from House et al, submitted).

Table D.1. Raw SCR data for H4 point mutants
Strains were constructed by SW and subsequent assays were performed by Nealia House as previously described (see Appendix A). An asterisk indicates a p-value < 0.05 compared to the wildtpe recombination rate (adapted from House et al, submitted).

Strain	H3/H4 WT	H4-K12R	H4K16R	H3/H4 WT + MMS	H4-K12R + MMS	H4K16R + MMS
	11.37	0.98	1.56	7.80	4.30	4.31
	11.57	8.61	3.38	3.76	3.58	5.14
		2.09	1.79	4.79	3.32	11.73
Mean Rate ($\times 10^{-5}$)	**11.47**	**3.89**	**2.24***	**5.45**	**3.74**	**7.06**

Appendix E. Chromatin Immunoprecipitation Information

Chromatin Immuoprecipitation

ChIP analysis was carried out by Nealia House as previously described (House et al, submitted 2014). ChIP was performed in alpha-factor synchronized cells with relevant antibodies for the protein of interest.

Resulting ChIP results of the Rsc1 and Rsc2 proteins are shown below (Figures E.1 and E.2). Previous ChIP lab data for H4-K16ac detection (not shown here) indicates that an enrichment of H4-K16 acetylation occurs roughly 20 minutes into S-phase. The peak in Rsc2 detection (Figure E.2) corresponds to the H4-K16ac peak, indicating that Rsc2 is physically recruited at the same time as this acetylation event. Rsc1 does not show the same characteristic peak (Figure E.1), suggesting that its role in H4-K16-dependent acetylation is not as strong. The later peak might also support the involvement of Rsc1 in repair pathways such as DSBR, which typically occur at later stages of S-phase.

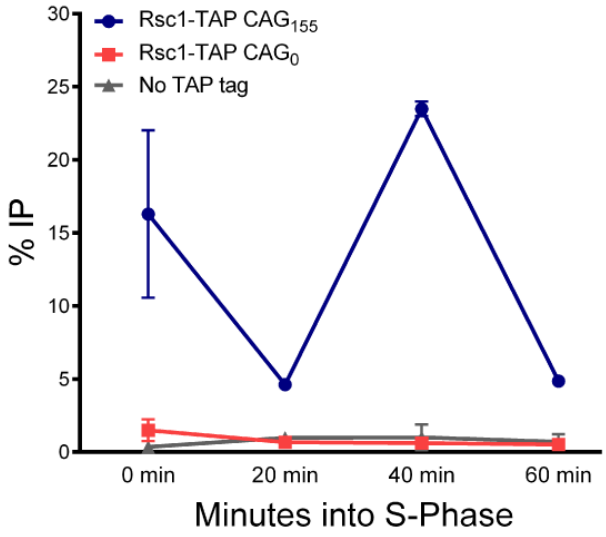

Figure E.1. Rsc1 is recruited to the CAG-repeat 40 minutes into S-phase
Detection by ChIP revealed a signal peak for Rsc1 40 minutes into S-phase. The late recruitment of Rsc1 to the CAG repeat suggests it is not recruited directly following H4-K16 acetylation, but may suggest a role in DSBR. ChIP analysis performed by Nealia House (adapted from House et al., submitted).

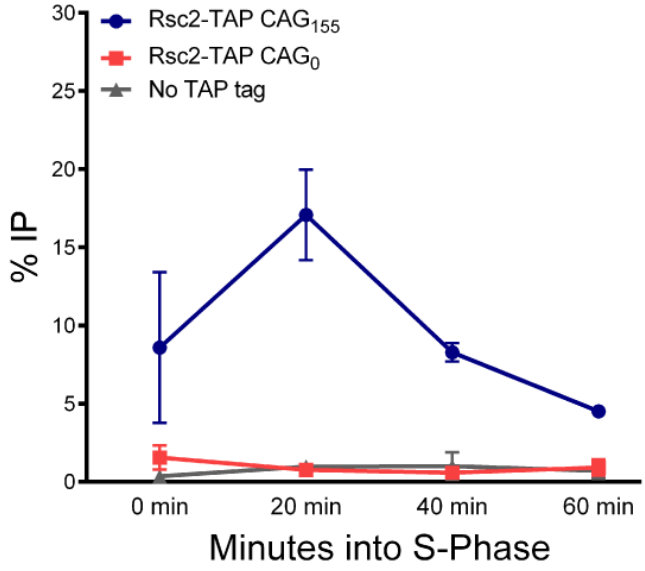

Figure E.2. Rsc2 is recruited to the CAG-repeat 20 minutes into S-phase
Detection by ChIP revealed a signal peak for Rsc2 20 minutes into S-phase. This peak corresponds to the timing of a previous ChIP study for H4-K16ac (not shown in this thesis). The corresponding peaks of H4-K16ac and Rsc2 suggest direct recruitment of Rsc2 to the CAG repeat by H4-K16 acetylation. ChIP analysis performed by Nealia House (adapted from House et al., submitted).

Appendix F. Additional Experimental Results

F.1 The Rad54 remodeler protein contributes to repeat stability, while the Fun30 protein may contribute to repeat stability

Rad54 is a remodeling protein involved in various stages of homologous recombination pathways (Heyer et al. 2006). Rad54 contains an ATPase domain that allows it to translocate along double stranded DNA (Ceballos and Heyer 2011). It functions as a remodeler due to its promotion of bidirectional branch migration of Holliday junctions (Bugreev et al. 2006). Additionally, Rad54 acts with Rad51 in nucleoprotein filament formation and strand invasion (Bugreev et al 2006; Heyer et al 2006). Thus, for its role in H4-mediated pathways and remodeling function, Rad54 was an attractive remodeler candidate to investigate for the model of DNA repair at the CAG repeat.

The Fun30 protein was another protein tested for epistasis with Esa1 and H4-targeting HDAC proteins. Fun30 is a Snf2-like protein that is found to remodel near centromeric and telomeric regions, and is found at DNA double strand breaks where it promotes strand resection (Seeber et al. 2013; Chen et al, 2012).

Strains constructed for this thesis include the *rad54*Δ and *hst1*Δ*hos2*Δ*sir2*Δ*fun30*Δ mutants (see Table B.1). The *esa1-1851 rad54*Δ and *hst1*Δ*hos2*Δ*sir2*Δ*rad54*Δ strains were constructed by Nealia House. The *esa1-1851 fun30*Δ and *hst1*Δ*hos2*Δ*sir2*Δ*fun30*Δ strains could not be constructed successfully after multiple transformation attempts. A complete study of Rad54 stability, including epistasis with Esa1 and HDAC proteins Hst1, Hos2, and Sir2, was carried out, as described in the next section, while only the Fun30 knockout studied was in the triple HDAC knockout background.

An increased expansion phenotype was observed for all Rad54 and Fun30 knockout strains although the *hst1Δhos2Δsir2Δrad54Δ* was not significantly elevated from the wildtype (see Figure F.1). Because Rad54 and Fun30 do not contain a bromodomain, and therefore would not be directly recruited by H4K16ac during repair, we did not pursue these proteins any further.

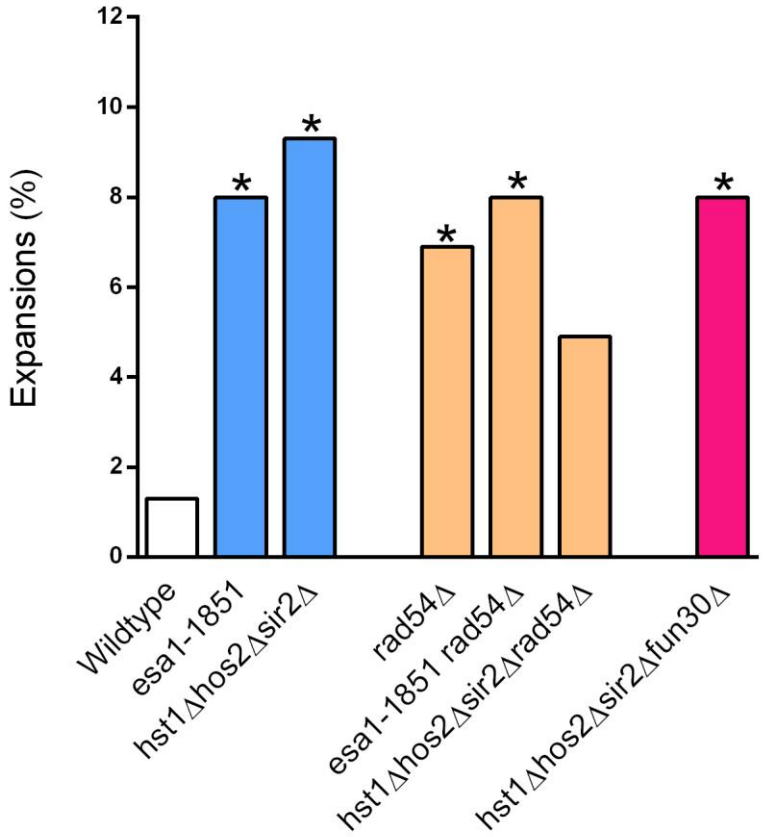

Figure F.1 Stability data for constructed Rad54 and Fun30 mutant strains
Stability assays for these knockout strains suggest Rad54 contributes to CAG repeat stability. The contribution of Rad54 appears to be epistatic with Esa1, but CAG expansions are slightly suppressed in the HDAC rad54Δ quadruple mutant. The Fun30 protein may be contributing to repeat stability, but a comparison to a single Fun30 deletion mutant is required to make this claim (not constructed). All assays performed by Nealia House.

F.2 Esa1 acetylation of Histone H4 does not contribute to chromosomal fragility

An *esa1-1851* strain with a $(CAG)_{155}$ tract was constructed in order to test if CAG repeat fragility was caused by the absence of Esa1 acetylation function. Fragility in an *esa1-1851* $(CAG)_{85}$ strain had previously been characterized, but for consistency in data to the $(CAG)_{155}$ tracts used in ChIP analysis, an additional strain with the same tract length was constructed.

The *esa1-1851* $(CAG)_{155}$ strain was constructed using the two-step gene replacement technique as previously described (see Methods section). Knockout cassettes were made from an *esa1-1851* (CFY2050) genomic template. Verification of the C304S mutation was verified by sequencing using the Esa1For39bp primer (CF primer #620).

In order to measure chromosomal breakage at the CAG-repeat in *esa1-1851* mutants (this study), a fragility assay was performed in which YAC breakage can be quantified. Fragility assays were performed as described in Sundararajan et al. (2010) with the following modifications: cultures were started in 1mL of YC-Leu at OD_{600} 0.04, and grown to a final OD_{600} between 1.5 and 2.5. Samples of 200µL of culture were plated on FOA-Leu plates and grown at 30°C for 3 days. An additional 100µL of culture from each culture was pooled in sets of ten for total cell counts. Total cell counts on YC-Leu (10^{-4} and 10^{-5} dilutions) were grown at 30°C for 3 days.

In both the *esa1-1851* $(CAG)_{85}$ strain and the *esa1-1851* $(CAG)_{155}$ strain, no increase in fragility was observed (see Figure F.2, Table F.1). This indicates that any double strand breaks that occur at the CAG repeat can be repaired in the *esa-1851* mutant. Further, this indirectly supports other evidence that H4 acetylation stimulates repair caused specifically by transient forms of damage, such as nicks, gaps, and hairpin formation.

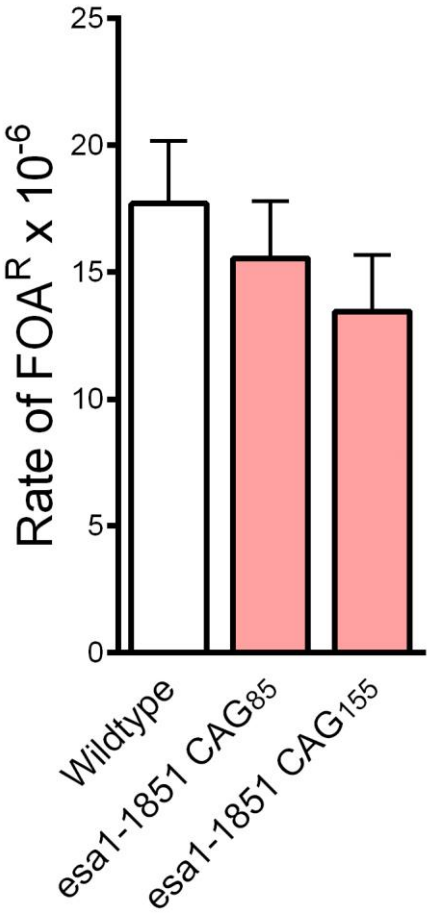

Figure F.2. Chromosomal fragility of *esa1-1851* mutants
The rates of chromosomal breakage were not different from wild-type in *esa1-1851* mutants with two different CAG-repeat tract lengths. This data provides evidence that H4 acetylation is not required for repair of DSBs at the CAG-repeat.

Table F.1. Raw Fragility Assay Data for *esa1-1851* mutant
Wildtype fragility assays were performed by previous Freudenreich lab undergraduate Jonathan Moy; *esa1-1851* $(CAG)_{85}$ fragility assays performed by Nealia House (adapted from Figure 4.E-1 Nealia House 2013).

Strain	**Rate of FOA^R (x 10^{-6})**						**Average Rate**
Wildtype $(CAG)_{85}$	20.0	9.5	17.4	10.2	19.8	25.3	18.9 x 10^{-6}
	0.36	12.5	27.3	26.7	28.7	29.5	
esa1-1851 $(CAG)_{85}$	13.2	17.5	13.3	14.4	25.6	9.41	15.6 x 10^{-6}
esa1-1851 $(CAG)_{155}$	17.8	8.1	11.5	16.4			13.4 x 10^{-6}

F.3 Acetylation of the H3 N-terminal tail does not contribute to repeat stability, but contribution of individual lysine residues is unknown

Previous data collected in the lab showed that an H3-*N*Δ mutant did not cause an increase in expansion phenotype, while lysine to arginine point mutants for histone H4 did show an increased expansion phenotype (see Figure 5 in Introduction). However, for a higher degree of consistency between data points (N-terminal deletions versus point mutants), we wanted to study the specific lysine residues on H3 when acetylation function is lost.

In order to construct a plasmid containing H3 lysine residues mutated to arginine residues, a system of site-directed mutagenesis was used. Plasmids containing the H3-K9,14,18,23,27R mutant sequence were constructed using the NEB Q5 Site-Directed Mutagenesis kit, according to the manufacturer's instructions. Primers were designed using the NEBaseChanger program by New England Biolabs, and are listed in Table F.2. The plasmid template used was a pRS314 plasmid with the copy 2 histone genes inserted into the multiple cloning site (CF plasmid #319, created by Jiahui Yang). The PCR used an annealing temperature of 67°C, as suggested by the NEBaseChanger program, and an extension time of 4 minutes, based on the suggested 30 seconds per kb of plasmid in the protocol (the plasmid was about 7.5kb). A visual representation of the site-directed mutagenesis system is given in Figure F.3. Successful bacterial transformants were mini-prepped using the Zymo Research Zyppy Plasmid MiniPrep kit, according to the manufacturer's instructions. Mutagenized plasmids were confirmed by sequencing, using universal sequencing primer T3, which anneals about 57bp downstream of the insert (see Figure F.4).

Table F.2. Primers used in Site-Directed Mutagenesis for creation of the H3-K9,14,18,23,27R plasmid

Primers were designed using the NEBaseChanger program by New England Biolabs. The nucleotides corresponding to a mismatch in the PCR amplification step of the mutagenesis are highlighted in yellow. Right primer corresponded to mutations in residues K23 and K27, while the Left primer accounted for mutations in residues (from left to right) K18, K14, and K9.

Primer Name	CF Primer Number	Sequence (5'→3')
H3_5KR_Right2	1425	ACAATTAGCCTCCAGGGCTGCCAGAAGATCCGCCCCATCTACCGGT
H3_5KR_Left2	1426	CTTCTTGGGGCTCTACCACCAGTGGATCTTCTAGCTGTTTGTTTAGTTCTGGCC

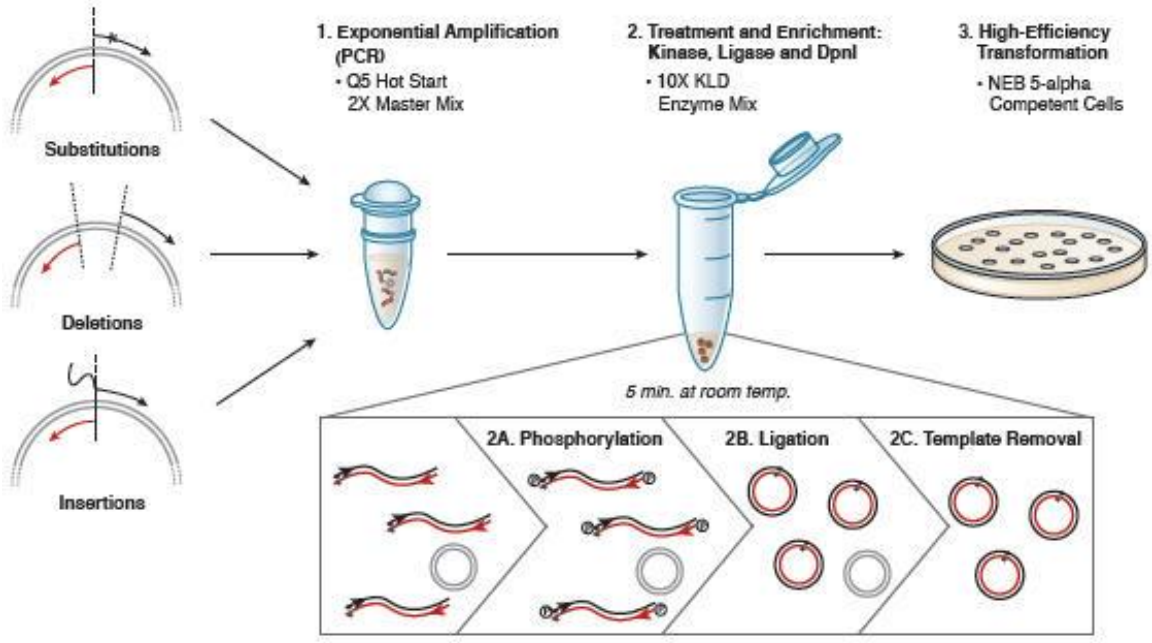

Figure F.3. Scheme for Q5 Site-Directed Mutagenesis Kit

In order to introduce substitutions, primers annealing to a plasmid template incorporate mismatches through a PCR amplification step (1). Next, PCR product was mixed with a buffer containing kinase enzymes (to phosphorylate the PCR products), ligase (to circularize the plasmid), and restriction enzyme DpnI, which specifically targets methylated DNA to selectively cleave the template plasmid (2). Finally, mutagenized plasmids are introduced to bacteria via heat-shock transformation (3). (Figure obtained from NEB website).

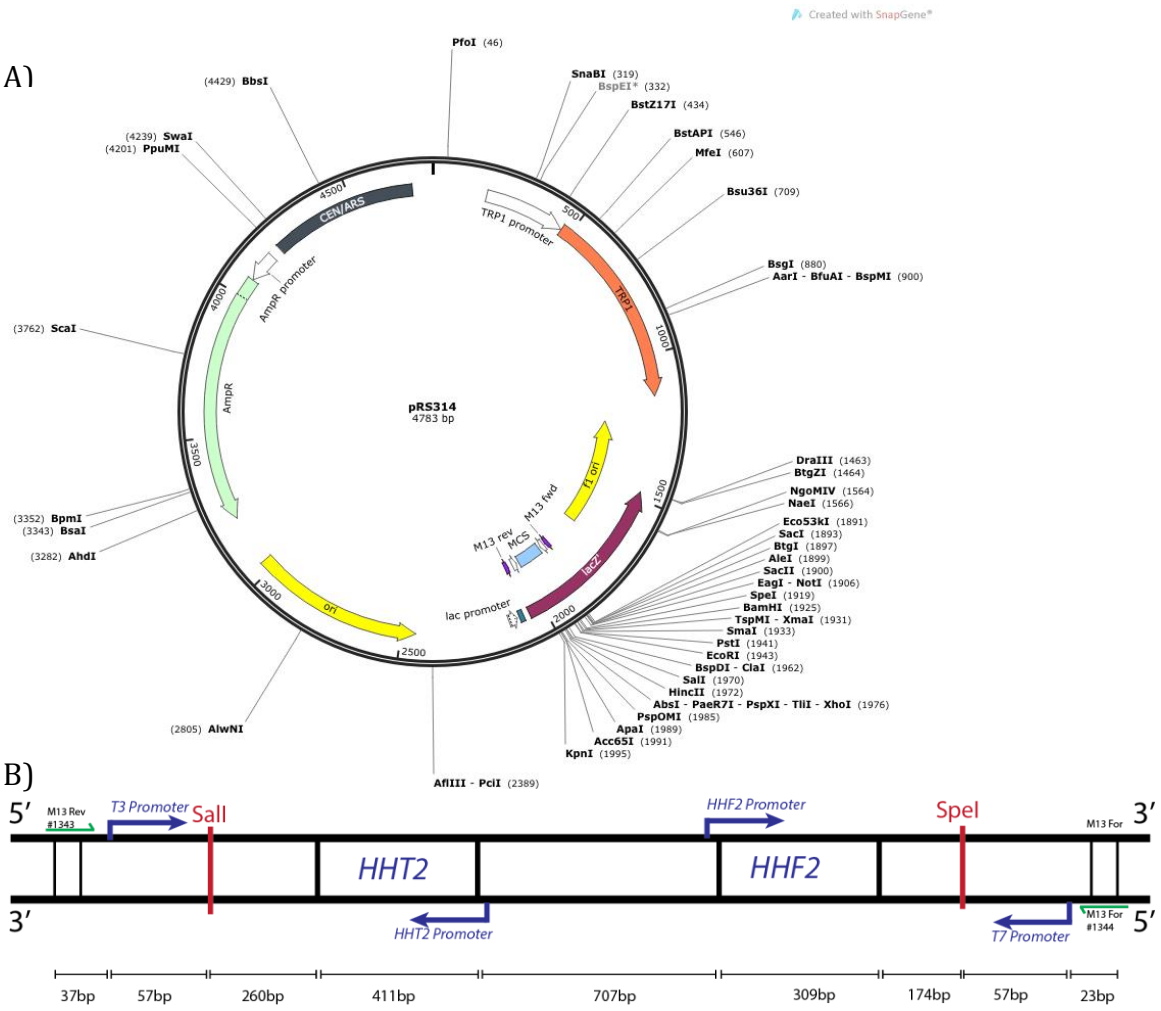

Figure F.4. Plasmid CF #319 has a pRS314 backbone and an *HHT2-HHF2* genomic locus insertion
The H3/H4 wildtype plasmid (CF plasmid #319, created by Jiahui Yang) is a Trp+, pRS314 backbone plasmid (A) (downloaded from SnapGene website). The genomic section of DNA from yeast chromosome XV containing the *HHT2-HHF2* genes is inserted between the SalI and SpeI cut sites (B). Promoter sequences, and other features of the plasmid are shown above.

To confirm yeast transformants by sequencing, a genomic DNA mini-prep was performed as previously described (see Methods section). An Expand PCR was performed using primers homologous to the plasmid sequence features M13 Forward and M13 Reverse in order to amplify the *HHT2* gene in the endogenous yeast plasmid (see Figure F.4). PCR product was then collected and purified using the Sigma-Aldrich Gen-Elute PCR Clean-Up Kit, according to

the manufacturer's instructions. Concentration of DNA was calculated from 1µL of the PCR sample using a ThermoScientific Nanodrop machine. Sequencing was performed by Macrogen, Inc., using the T3 universal sequencing primer in their sequencing reaction.

At the time of this paper's writing, the correct mutation has not been confirmed in yeast by sequencing. Attempts to sequence this mutant either resulted in Stability assays for this mutant will be performed once the correct mutation sequence is confirmed in yeast.

Works Cited

Altaf, M., Auger, A., Monnet-Saksouk, J., Brodeur, J., Piquet, S., Cramet, M., . . . Cote, J. (2010). NuA4-dependent acetylation of nucleosomal histones H4 and H2A directly stimulates incorporation of H2A.Z by the SWR1 complex. *The Journal of biological chemistry, 285*(21), 15966-15977. doi: 10.1074/jbc.M110.117069 [doi]

Andersen, P. L., Xu, F., & Xiao, W. (2008). Eukaryotic DNA damage tolerance and translesion synthesis through covalent modifications of PCNA. *Cell research, 18*(1), 162-173. doi: cr2007114 [pii]

Aparicio, O., Geisberg, J. V., Sekinger, E., Yang, A., Moqtaderi, Z., & Struhl, K. (2005). Chromatin immunoprecipitation for determining the association of proteins with specific genomic sequences in vivo. *Current protocols in molecular biology / edited by Frederick M.Ausubel ...[et al.], Chapter 21*, Unit 21.23. doi: 10.1002/0471142727.mb2103s69 [doi]

Ataian, Y., & Krebs, J. E. (2006). Five repair pathways in one context: chromatin modification during DNA repair. *Biochemistry and cell biology = Biochimie et biologie cellulaire, 84*(4), 490-504. doi: o06-075 [pii]

Bird, A. W., Yu, D. Y., Pray-Grant, M. G., Qiu, Q., Harmon, K. E., Megee, P. C., . . . Christman, M. F. (2002). Acetylation of histone H4 by Esa1 is required for DNA double-strand break repair. *Nature, 419*(6905), 411-415. doi: 10.1038/nature01035 [doi]

Bugreev, D. V., Mazina, O. M., & Mazin, A. V. (2006). Rad54 protein promotes branch migration of Holliday junctions. *Nature, 442*(7102), 590-593. doi: nature04889 [pii]

Ceballos, S. J., & Heyer, W. D. (2011). Functions of the Snf2/Swi2 family Rad54 motor protein in homologous recombination. *Biochimica et biophysica acta, 1809*(9), 509-523. doi: 10.1016/j.bbagrm.2011.06.006 [doi]

Chai, B., Huang, J., Cairns, B. R., & Laurent, B. C. (2005). Distinct roles for the RSC and Swi/Snf ATP-dependent chromatin remodelers in DNA double-strand break repair. *Genes & development, 19*(14), 1656-1661. doi: 19/14/1656 [pii]

Chambers, A. L., Brownlee, P. M., Durley, S. C., Beacham, T., Kent, N. A., & Downs, J. A. (2012). The two different isoforms of the RSC chromatin remodeling complex play distinct roles in DNA damage responses. *PloS one, 7*(2), e32016. doi: 10.1371/journal.pone.0032016 [doi]

Chen, X., Cui, D., Papusha, A., Zhang, X., Chu, C. D., Tang, J., . . . Ira, G. (2012). The Fun30 nucleosome remodeller promotes resection of DNA double-strand break ends. *Nature, 489*(7417), 576-580. doi: 10.1038/nature11355 [doi]

Chittuluru, J. R., Chaban, Y., Monnet-Saksouk, J., Carrozza, M. J., Sapountzi, V., Selleck, W., . . . Asturias, F. J. (2011). Structure and nucleosome interaction of the yeast NuA4 and Piccolo-NuA4 histone acetyltransferase complexes. *Nature structural & molecular biology, 18*(11),

1196-1203. doi: 10.1038/nsmb.2128 [doi]

Choy, J. S., & Kron, S. J. (2002). NuA4 subunit Yng2 function in intra-S-phase DNA damage response. *Molecular and cellular biology, 22*(23), 8215-8225.

Costelloe, T., Fitzgerald, J., Murphy, N. J., Flaus, A., & Lowndes, N. F. (2006). Chromatin modulation and the DNA damage response. *Experimental cell research, 312*(14), 2677-2686. doi: S0014-4827(06)00254-0 [pii]

Decker, P. V., D. Y. Yu, M. Iizuka, Q. Qiu, and M. M. Smith. "Catalytic-Site Mutations in the MYST Family Histone Acetyltransferase Esa1."Genetics 178.3 (2008): 1209-220. Print.

Debacker, K., Frizzell, A., Gleeson, O., Kirkham-McCarthy, L., Mertz, T., & Lahue, R. S. (2012). Histone deacetylase complexes promote trinucleotide repeat expansions. *PLoS biology, 10*(2), e1001257. doi: 10.1371/journal.pbio.1001257 [doi]

Durant, M., & Pugh, B. F. (2007). NuA4-directed chromatin transactions throughout the Saccharomyces cerevisiae genome. *Molecular and cellular biology, 27*(15), 5327-5335. doi: MCB.00468-07 [pii]

Filippakopoulos, P., & Knapp, S. (2012). The bromodomain interaction module. *FEBS letters, 586*(17), 2692-2704. doi: 10.1016/j.febslet.2012.04.045 [doi]

Freudenreich, C. H. (2007). Chromosome fragility: molecular mechanisms and cellular consequences. *Frontiers in bioscience : a journal and virtual library, 12*, 4911-4924. doi: 2437 [pii]

Gangavarapu, V., Santa Maria, S. R., Prakash, S., & Prakash, L. (2011). Requirement of replication checkpoint protein kinases Mec1/Rad53 for postreplication repair in yeast. *mBio, 2*(3), e00079-00011. doi: 10.1128/mBio.00079-11 [doi]

Heyer, W. D., Li, X., Rolfsmeier, M., & Zhang, X. P. (2006). Rad54: the Swiss Army knife of homologous recombination? *Nucleic acids research, 34*(15), 4115-4125. doi: gkl481 [pii]

Horn, P. J., & Peterson, C. L. (2001). The bromodomain: a regulator of ATP-dependent chromatin remodeling? *Frontiers in bioscience : a journal and virtual library, 6*, D1019-1023.

Kim, J. C., & Mirkin, S. M. (2013). The balancing act of DNA repeat expansions. *Current opinion in genetics & development, 23*(3), 280-288. doi: 10.1016/j.gde.2013.04.009 [doi]

Kimura, A., Umehara, T., & Horikoshi, M. (2002). Chromosomal gradient of histone acetylation established by Sas2p and Sir2p functions as a shield against gene silencing. *Nature genetics, 32*(3), 370-377. doi: 10.1038/ng993 [doi]

Krogan, N. J., Baetz, K., Keogh, M. C., Datta, N., Sawa, C., Kwok, T. C., . . . Greenblatt, J. F. (2004). Regulation of chromosome stability by the histone H2A variant Htz1, the Swr1 chromatin

remodeling complex, and the histone acetyltransferase NuA4. *Proceedings of the National Academy of Sciences of the United States of America, 101*(37), 13513-13518. doi: 10.1073/pnas.0405753101 [doi]

Lenzmeier, B. A., & Freudenreich, C. H. (2003). Trinucleotide repeat instability: a hairpin curve at the crossroads of replication, recombination, and repair. *Cytogenetic and genome research, 100*(1-4), 7-24. doi: 72836 [doi]

Lowndes N.F., Toh G.W., DNA repair: the importance of phosphorylating histone H2AX, Curr. Biol. 15 (2005) R99–R102.

Kerrest, A., Anand, R. P., Sundararajan, R., Bermejo, R., Liberi, G., Dujon, B., . . . Richard, G. F. (2009). SRS2 and SGS1 prevent chromosomal breaks and stabilize triplet repeats by restraining recombination. *Nature structural & molecular biology, 16*(2), 159-167. doi: 10.1038/nsmb.1544 [doi]

McMurray, C. T. (1999). DNA secondary structure: a common and causative factor for expansion in human disease. *Proceedings of the National Academy of Sciences of the United States of America, 96*(5), 1823-1825.

Millar, C. B., & Grunstein, M. (2006). Genome-wide patterns of histone modifications in yeast. *Nature reviews.Molecular cell biology, 7*(9), 657-666. doi: nrm1986 [pii]

Mirkin, S. M. (2007). Expandable DNA repeats and human disease. *Nature, 447*(7147), 932-940. doi: nature05977 [pii]

Mizuguchi, G., Shen, X., Landry, J., Wu, W. H., Sen, S., & Wu, C. (2004). ATP-driven exchange of histone H2AZ variant catalyzed by SWR1 chromatin remodeling complex. *Science (New York, N.Y.), 303*(5656), 343-348. doi: 10.1126/science.1090701 [doi]

Mozlin, A. M., Fung, C. W., & Symington, L. S. (2008). Role of the Saccharomyces cerevisiae Rad51 paralogs in sister chromatid recombination. *Genetics, 178*(1), 113-126. doi: 10.1534/genetics.107.082677 [doi]

Nag, D. K., Suri, M., & Stenson, E. K. (2004). Both CAG repeats and inverted DNA repeats stimulate spontaneous unequal sister-chromatid exchange in Saccharomyces cerevisiae. *Nucleic acids research, 32*(18), 5677-5684. doi: 32/18/5677 [pii]

Niimi, A., Chambers, A. L., Downs, J. A., & Lehmann, A. R. (2012). A role for chromatin remodellers in replication of damaged DNA. *Nucleic acids research, 40*(15), 7393-7403. doi: 10.1093/nar/gks453 [doi]

Raisner, R. M., Hartley, P. D., Meneghini, M. D., Bao, M. Z., Liu, C. L., Schreiber, S. L., . . . Madhani, H. D. (2005). Histone variant H2A.Z marks the 5' ends of both active and inactive genes in euchromatin. *Cell, 123*(2), 233-248. doi: S0092-8674(05)01025-1 [pii]

Seeber, A., Hauer, M., & Gasser, S. M. (2013). Nucleosome remodelers in double-strand break repair. *Current opinion in genetics & development, 23*(2), 174-184. doi: 10.1016/j.gde.2012.12.008 [doi]

Shroff, R., Arbel-Eden, A., Pilch, D., Ira, G., Bonner, W. M., Petrini, J. H., . . . Lichten, M. (2004). Distribution and dynamics of chromatin modification induced by a defined DNA double-strand break. *Current biology : CB, 14*(19), 1703-1711. doi: 10.1016/j.cub.2004.09.047 [doi]

Smith, E. R., Eisen, A., Gu, W., Sattah, M., Pannuti, A., Zhou, J., . . . Allis, C. D. (1998). ESA1 is a histone acetyltransferase that is essential for growth in yeast. *Proceedings of the National Academy of Sciences of the United States of America, 95*(7), 3561-3565.

Sundararajan, R., Gellon, L., Zunder, R. M., & Freudenreich, C. H. (2010). Double-strand break repair pathways protect against CAG/CTG repeat expansions, contractions and repeat-mediated chromosomal fragility in Saccharomyces cerevisiae. *Genetics, 184*(1), 65-77. doi: 10.1534/genetics.109.111039 [doi]

Tamburini, B. A., & Tyler, J. K. (2005). Localized histone acetylation and deacetylation triggered by the homologous recombination pathway of double-strand DNA repair. *Molecular and cellular biology, 25*(12), 4903-4913. doi: 25/12/4903 [pii]

Turnpenny, P. & Ellard, S. (2005). Emery's Elements of Medical Genetics, 12th. ed. Elsevier, London.

van Attikum, H., & Gasser, S. M. (2005). The histone code at DNA breaks: a guide to repair? *Nature reviews.Molecular cell biology, 6*(10), 757-765. doi: nrm1737 [pii]

Wang, A., Kurdistani, S. K., & Grunstein, M. (2002). Requirement of Hos2 histone deacetylase for gene activity in yeast. *Science (New York, N.Y.), 298*(5597), 1412-1414. doi: 10.1126/science.1077790 [doi]

Wang, Y. H., Amirhaeri, S., Kang, S., Wells, R. D., & Griffith, J. D. (1994). Preferential nucleosome assembly at DNA triplet repeats from the myotonic dystrophy gene. *Science (New York, N.Y.), 265*(5172), 669-671.

Wu, W. H., Wu, C. H., Ladurner, A., Mizuguchi, G., Wei, D., Xiao, H., Wu, C. (2009). N terminus of Swr1 binds to histone H2AZ and provides a platform for subunit assembly in the chromatin remodeling complex. *The Journal of biological chemistry, 284*(10), 6200-6207. doi: 10.1074/jbc.M808830200 [doi]

Yu, Y., Deng, Y., Reed, S. H., Millar, C. B., & Waters, R. (2013). Histone variant Htz1 promotes histone H3 acetylation to enhance nucleotide excision repair in Htz1 nucleosomes. *Nucleic acids research, 41*(19), 9006-9019. doi: 10.1093/nar/gkt688 [doi]

Zeng, L., & Zhou, M. M. (2002). Bromodomain: an acetyl-lysine binding domain. *FEBS letters, 513*(1), 124-128. doi: S0014579301033099 [pii]

Zhang, H., & Lawrence, C. W. (2005). The error-free component of the RAD6/RAD18 DNA damage tolerance pathway of budding yeast employs sister-strand recombination. *Proceedings of the National Academy of Sciences of the United States of America, 102*(44), 15954-15959. doi: 0504586102 [pii]